ous solutions) that are preferable for pharmaceutical formulations (Arakawa et al., 2007).

The purpose of this study was to systematically examine the physical properties and protein-stabilizing effects of oligosaccharide-derived sugar alcohols for their application in freeze-dried formulations. It has been established that various sugar alcohols (e.g., sorbitol, xylitol, lactitol) protect proteins from heat-induced denaturation in aqueous solutions through a thermodynamic mechanism (preferential exclusion) identical to that of saccharides and other polyols (e.g., glycerol) (Arakawa and Timasheff, 1982; Gekko, 1982). Some pentitols and hexitols (e.g., xylitol, sorbitol) protect biological macromolecules (e.g., proteins) and microorganisms from inactivation and/or viability loss during freeze-thawing and during freeze-drying (Tamoto et al., 1961; Carpenter and Crowe, 1988). Varied physical properties (i.e., crystallinity, molecular mobility) have been considered as key factors that determine effects of sugar alcohols to stabilize proteins in frozen solutions and freeze-dried solids (Griebenow and Klibanov, 1995; Carrasquillo et al., 2000; Liao et al., 2002). For example, high propensity to crystallize in the frozen solution (e.g., mannitol) or to collapse during primary drying (e.g., sorbitol, xylitol) makes them inappropriate for main stabilizer in freeze-drying. Some oligosaccharide-derived sugar alcohols (e.g., maltitol, lactitol, maltotriitol) should have greater opportunities to structurally and kinetically stabilize proteins during freeze-drying and subsequent storage. Maltitol and lactitol are popular excipients for oral (tablet) formulations, and are also widely used in food industries as glass-forming additives upon cooling of edible hot-melt compositions (Slade et al., 2006). Information on the physical properties (e.g., thermal transition temperatures) and protein-stabilizing effects (e.g., enzyme activity, protein secondary structure) should be relevant in the application of sugar alcohols to the freeze-dried formulations.

2. Materials and methods

2.1. Materials

All chemicals employed in this study were of analytical grades and were obtained from the following commercial sources: L-lactic dehydrogenase (LDH, rabbit muscle), bovine serum albumin (BSA, essentially fatty acid free), glucose, trehalose dihydrate, sorbitol, and sucrose (Sigma Chemical, St. Louis, MO); maltitol, maltotriitol and maltotetraitol (Hayashibara Biochemical Laboratories, Okayama, Japan); maltose, lactose, mannitol, xylitol, lactitol monohydrate, and other chemicals (Wako Pure Chemical, Osaka, Japan); methanol dehydrate (Kanto Kagaku, Tokyo, Japan). The protein solutions were dialyzed against 50 mM sodium phosphate buffer (pH 7.0), and then centrifuged (1500 g × 5 min) and filtered (0.45 μm PVDF filters, Millipore, Bedford, MA) to remove insoluble aggregates before the freeze-drying study.

2.2. Freeze-drying

A freeze-drier (FreeZone-6; Labconco, Kansas City, MO) was used for lyophilization. Aliquots (0.3 ml) of aqueous solutions in flat-bottom glass vials (13 mm diameter, SVF-3; Nichiden-Rika Glass, Kobe, Japan) were placed on the shelf of the lyophilizer. The shelf was cooled to −40 °C at 0.5 °C/min, and then maintained at this temperature for 2 h before the primary drying process. The frozen solutions were dried under a vacuum (4.0 Pa) while maintaining the shelf temperature at −40 °C for 15 h, −30 °C for 6 h, and 35 °C for 6 h. The shelf was heated at 0.2 °C/min between the thermal steps. The vials were closed with rubber stoppers under a vacuum.

2.3. Thermal analysis

Thermal analysis of frozen solutions and dried solids was performed by using a differential scanning calorimeter (Q-10; TA Instruments, New Castle, DE) and software (Universal Analysis 2000; TA Instruments). Aliquots of aqueous solutions (10 μl) in hermetic aluminum cells were cooled from room temperature to −70 °C at 10 °C/min, and then scanned by heating at 5 °C/min. Freeze-dried solids (1–2 mg) in hermetic aluminum cells were subjected to the thermal analysis from −20 °C at 5 °C/min under a nitrogen gas flow. Cooled-melt saccharide and sugar alcohol solids obtained by a brief period of heating (1 min at 160 °C for maltose monohydrate, xylitol, sorbitol, maltitol, and lactitol monohydrate; at 180 °C for glucose; at 200 °C for sucrose, mannitol, and maltotriitol; and at 220 °C for lactose and trehalose monohydrate) and subsequent rapid cooling (−50 °C) in hermetic aluminum cells were scanned at 5 °C/min to obtain the glass transition temperatures. The glass transition temperatures were determined as the maximum inflection point of the discontinuities in the heat flow curves.

2.4. Freeze-drying microscopy (FDM)

We observed the behavior of frozen aqueous excipient solutions under a vacuum using a freeze-drying microscope system (Lyostat2; Biopharma Technology, Winchester, UK) with an optical microscope (BX51; Olympus, Tokyo). Aqueous solutions (2 μl) sandwiched between cover slips (70 μm apart) were frozen at −40 °C and then maintained at that temperature for 5 min. Each sample was heated under a vacuum (12.9 Pa) at 5 °C/min to a temperature approximately 5 °C below its T_g' as obtained by thermal analysis, and then scanned at an angle speed of 1 °C/min after reaching T_g'. The collapse onset temperature (T_c) of the frozen solution was determined from the first appearance of translucent dots behind the ice sublimation interface ($n = 3$).

2.5. Powder X-ray diffraction (XRD) and residual water measurements

The powder X-ray diffraction patterns were measured at room temperature by using a Rint-Altima diffractometer (Rigaku, Tokyo, Japan) with Cu Kα radiation at 40 kV/40 mA. The samples were scanned in the area of $5° < 2\theta < 35°$ at an angle speed of 5°/min. The lyophilized solids were suspended in dehydrated methanol to obtain residual water by a volumetric Karl-Fischer titrator (AQV-6; Hiranuma Sangyo, Ibaraki, Japan). Residual water contents were shown as ratios (%) to the estimated solid weights in the vials.

2.6. Freeze-drying and activity measurement of LDH

Aqueous solutions (0.5 ml) containing LDH (0.05 mg/ml), excipients (100 mg/ml) and sodium phosphate buffer (50 mM, pH 7.0) were lyophilized in the flat-bottom glass vials. Some freeze-dried solids plugged with rubber stoppers were stored at 50 °C for 7 days in a temperature chamber (Model SH-221, Espec, Osaka, Japan). Pyruvate and NADH were used as substrates to obtain LDH activity from the absorbance reduction at 340 nm (25 °C). Residual enzyme activity was shown as the ratio (%) to that of the solution before freezing ($n = 6$) (Izutsu et al., 1994).

2.7. Fourier-transform infrared (FT-IR) analysis of freeze-dried BSA

A Fourier-transform infrared spectrophotometer (MB-104; Bomen, Quebec, Canada) with a dry gas generator (Balston, Haverhill, MA) and software (PROTA; BioTools, Jupiter, FL and GRAMS/32; Galactic Ind., Salem, NH) was used to obtain mid-infrared spectra of

Table 1
Physical properties of saccharides and sugar alcohols in frozen solutions and freeze-dried solids.

	Excipient				Excipient + BSA + Buffer		
	Frozen solution	Freeze-dried solid		Cooled-melt Solid	Frozen solution	Freeze-dried solid	
	T_g' (°C)	T_g (°C)	Residual water (%, w/w)	T_g (°C)	T_g' (°C)	T_g (°C)	Residual\water (%, w/w)
w/o excipients					n.d.	n.d.	6.3 ± 0.4
Glucose	−42.7 ± 0.5	Collapsed	–	37.3 ± 0.8	−41.4 ± 1.6	41.5 ± 2.0	2.6 ± 0.4
Lactose	−29.1 ± 0.1	90.9 ± 6.6	1.2 ± 0.1	112.0 ± 1.9	−27.8 ± 1.8	105.3 ± 2.2	1.0 ± 0.4
Sucrose	−33.5 ± 0.1	62.0 ± 2.6	1.8 ± 0.9	46.4 ± 0.3	−32.0 ± 0.7	68.2 ± 0.8	1.9 ± 0.0
Maltose monohydrate	−31.1 ± 0.0	86.2 ± 1.1	0.9 ± 0.0	68.8 ± 1.5	−28.8 ± 1.6	95.6 ± 1.2	1.2 ± 0.4
Trehalose dihydrate	−30.6 ± 0.1	80<	1.0 ± 0.2	117.3 ± 0.3	−27.4 ± 0.5	90<	1.2 ± 0.4
Xylitol	−48.5 ± 0.5	Collapsed	–	−21.9 ± 0.2	−45.9 ± 1.2	Collapsed	–
Sorbitol	−45.0 ± 0.4	Collapsed	–	−1.9 ± 0.2	−39.9 ± 0.7	Collapsed	–
Mannitol	Crystallized	Crystallized	–	Crystallized	Crystallized	Partially Crystallized	–
Maltitol	−36.7 ± 0.2	40.6 ± 0.4	1.1 ± 1.1	47.3 ± 0.8	−35.7 ± 0.6	56.3 ± 1.0	1.3 ± 0.4
Lactitol monohydrate	−31.8 ± 0.1	54.9 ± 2.5	0.3 ± 0.5	48.4 ± 3.3	−29.2 ± 1.5	63.3 ± 1.9	1.2 ± 0.2
Maltotriitol	−29.5 ± 0.0	72.8 ± 2.8	0.3 ± 0.2	88.6 ± 0.8	−26.6 ± 0.7	85.3 ± 3.1	1.5 ± 0.2
Maltotetraitol	−24.9 ± 0.2	n.d.	1.2 ± 0.3	–	−24.8 ± 0.3	n.d.	0.9 ± 0.1

Average ± s.d. (n = 3).

BSA in the aqueous solution and freeze-dried solids (Prestrelski et al., 1993; Dong et al., 1995; Izutsu et al., 2004). Spectra of aqueous BSA solutions (10 mg/ml in 50 mM sodium phosphate buffer, pH 7.0) were recorded at 4 cm^{-1} resolution using infrared cells with CaF_2 windows and 6 μm film spacers (256 scans). Spectra of freeze-dried BSA solids were obtained from pressed disks containing the sample (approximately 1 mg BSA) and dried potassium bromide (approx. 250 mg). Area-normalized second-derivative amide I spectra (1600–1715 cm^{-1}, 7-point smoothing) were employed to elucidate the integrity of the protein secondary structure.

2.8. Non-enzymatic color development of freeze-dried solids

Lyophilized solids containing L-lysine (5 mg/ml) and a saccharide or a sugar alcohol (100 mg/ml, 0.3 ml) were stored at 80 °C for 4 days. Changes in the absorbance (280 nm) of the re-hydrated solutions (5-times diluted) were obtained by using a UV–visible spectrophotometer (UV-2450; Shimadzu, Kyoto, Japan).

3. Results

3.1. Physical property of frozen solutions

Most of the frozen aqueous solutions containing a saccharide or a sugar alcohol (100 mg/ml) showed typical thermograms that indicated an amorphous freeze-concentrated phase surrounding ice crystals (Table 1). An increase in the solute molecular weight shifted the glass transition of the maximally freeze-concentrated phase (T_g') to higher temperatures, which trend was consistent with literature (Levine and Slade, 1988). Addition of BSA (10 mg/ml) and sodium phosphate buffer (50 mM, pH 7.0) raised the T_g' of the frozen excipient solutions except for that of maltotetraitol. The frozen mannitol solution showed an exotherm peak that indicated eutectic crystallization at around −23 °C (Cavatur et al., 2002).

Freeze-drying of some disaccharides or oligosaccharide-derived sugar alcohol solutions (trehalose, sucrose, maltitol, lactitol, maltotriitol) resulted in cake-structure solids. Conversely, frozen solutions containing smaller solute molecules (e.g., glucose, sorbitol, xylitol, T_g' < −40 °C) collapsed during the process. Addition of BSA prevented glucose from physical collapse during the freeze-drying process. Freeze-drying microscopy indicated dynamic changes of frozen solutions under vacuum (Fig. 1). Heating of a frozen lactitol solution showed ice sublimation from the upper right corner of the image, leaving a structurally ordered dark dried region behind (−30 °C). Further heating induced transparent dots that indicated loss of the local structure (collapse onset temperature, T_c: −27.8 ± 0.3 °C), followed by larger structural damage. Other frozen solutions also showed T_cs (trehalose: −24.3 ± 0.7 °C; maltitol: −31.2 ± 2.1 °C) several degrees higher than their T_g's.

3.2. Characterization of freeze-dried solids

The physical properties of the freeze-dried solids were studied by thermal analysis, powder X-ray diffraction, and residual water measurement. Thermal analysis showed glass transition of some lyophilized oligosaccharide-derived sugar alcohol solids (maltitol, lactitol, maltotriitol) at above room temperature (Table 1) (Shirke et al., 2005). No apparent transition was observed in freeze-dried maltotetraitol solid. Some freeze-dried disaccharides (e.g., lactose, maltose) showed T_gs higher than those of the structurally relating sugar alcohols. Freeze-dried solids containing BSA, buffer components, and disaccharides or oligosaccharide-derived sugar alcohols (maltitol, lactitol, maltotriitol) showed halo powder X-ray diffraction (XRD) patterns typical for non-crystalline solids (Fig. 2). Some peaks in the XRD pattern, as well as the combination of an exotherm peak (51.7 °C) and an exotherm peak (164.1 °C) in the thermogram, indicated partially crystallized mannitol lyophilized with BSA and the buffer salts. The small peaks in the XRD patterns also suggested partial crystallization of glucose and sorbitol during the freeze-drying process and/or during sample preparation for the analysis. The residual water contents of the cake-structure dried solids were less than 2%. The protein lyophilized without the stabilizing excipients showed higher residual water contents.

3.3. Effects on protein stability

The effects of the oligosaccharide-derived sugar alcohols on the protein stability during the freeze-drying process and subsequent storage were studied through the enzyme activity (LDH) and secondary structure (BSA) measurements. The enzyme (0.05 mg/ml) freeze-dried from the sodium phosphate buffer solution (50 mM, pH 7.0) retained approximately 60% of its initial activity (Fig. 3). The disaccharides and oligosaccharide-derived sugar alcohols (100 mg/ml sucrose, trehalose, maltitol, lactitol, maltotriitol) protected LDH from the activity loss during freeze-drying. In contrast, sorbitol and mannitol did not show any apparent effect on the co-lyophilized enzyme activity. The enzyme lyophilized with sorbitol or in the absence of polyols lost most of its activity during storage at 50 °C for 7 days. The disaccharides and oligosaccharide-

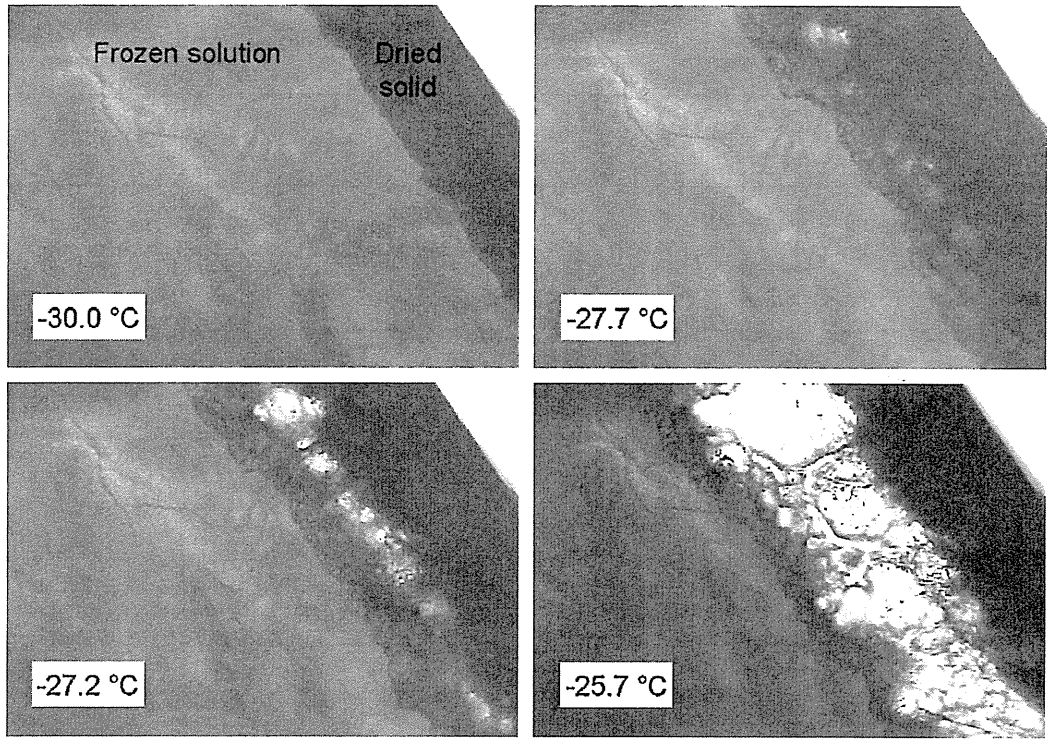

Fig. 1. Freeze-drying microscopy images of a frozen lactitol solution (100 mg/ml) obtained during a heating scan (1 °C/min). The frozen solution (2 μl) in a thin cell was dried under a vacuum (12.9 Pa) from the upper right corner of the figures.

derived sugar alcohols retained the enzyme activity during the high-temperature storage. The freeze-dried maltitol formulation shrunk during the storage near its glass transition temperature. The enzyme lyophilized with mannitol retained its activity to some extent in the largely crystallized solid during the high-temperature storage.

The effects of the saccharides and sugar alcohols on the secondary structure of freeze-dried BSA were studied (Fig. 4). The area-normalized second-derivative amide I spectra of BSA in the sodium phosphate buffer solution (50 mM, pH 7.0) showed a large band at 1656 cm^{-1} that denoted a predominant α-helix structure in the native conformation (Dong et al., 1995). Lyophilization of the protein from the buffer resulted in a reduction of the α-helix band intensity and broadened the overall spectra, indicating a perturbed secondary structure (Prestrelski et al., 1993). Maltitol and

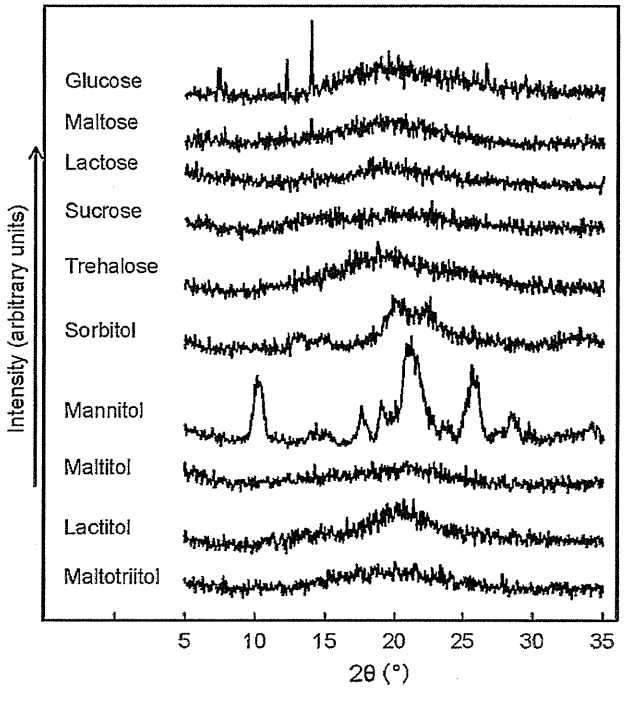

Fig. 2. Powder X-ray diffraction patterns of solids freeze-dried from solutions containing BSA (10 mg/ml), excipient (100 mg/ml) and sodium phosphate buffer (50 mM, pH 7.0).

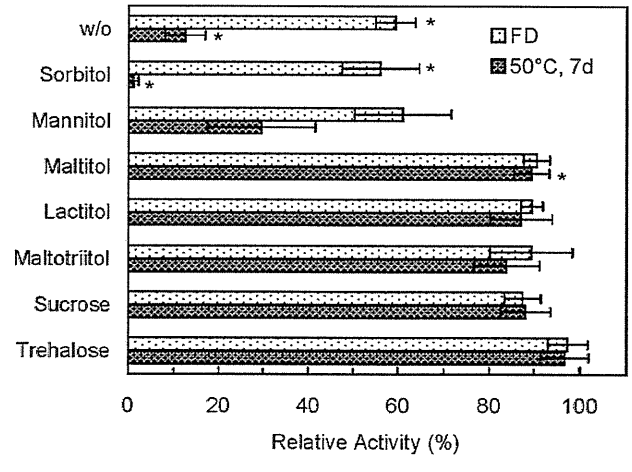

Fig. 3. Effects of excipients on the relative activity of rabbit muscle lactate dehydrogenase after freeze-drying and subsequent storage at 50 °C for 7 days ($n = 3$). Aqueous solutions containing LDH (0.05 mg/ml), excipient (100 mg/ml) and sodium buffer salt (50 mM, pH 7.0) were freeze-dried in glass vials. Asterisks indicate collapsed or shrunk solids.

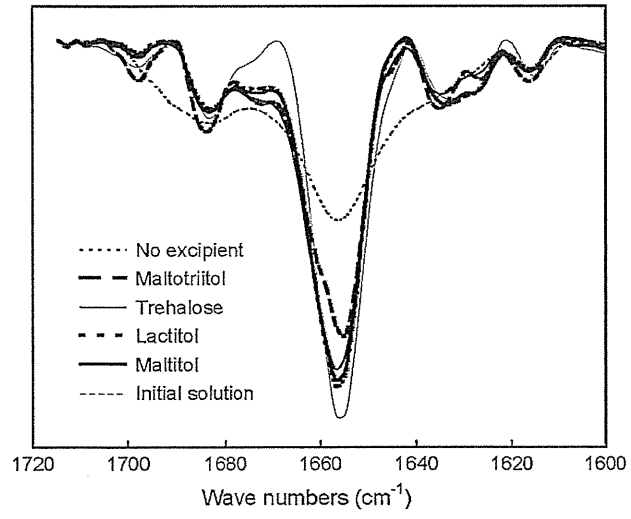

Fig. 4. Area-normalized second-derivative amide I spectra of BSA (10 mg/ml) in a sodium phosphate buffer solution (50 mM, pH 7.0) and in solids freeze-dried with or without co-solutes (100 mg/ml).

lactitol were as effective as trehalose at retaining the conformation of the co-lyophilized protein. The smaller α-helix band of the protein lyophilized with maltotriitol suggested insufficient structure stabilization.

3.4. Chemical stability in freeze-dried solids

The possible reactivity of the sugar alcohols with proteins (e.g., Maillard reaction) in the dried solids was studied by using model freeze-dried systems containing the excipients and L-lysine (Fig. 5) (Kawai et al., 2004). The co-lyophilized solids maintained the cake-structure (e.g., trehalose, lactose) or shrunk (other excipients) during the storage at an elevated temperature (80 °C for 4 days). The solids turned brown to varying degrees irrespective of the solid structure. The high-temperature storage of solids containing the reducing saccharides (glucose, maltose, lactose) and L-lysine induced apparent absorbance changes of the re-hydrated solutions (3 < Abs.280, data not shown). The oligosaccharide-derived sugar alcohols (maltitol, lactitol, maltotriitol) showed lower chemical reactivity with co-lyophilized L-lysine

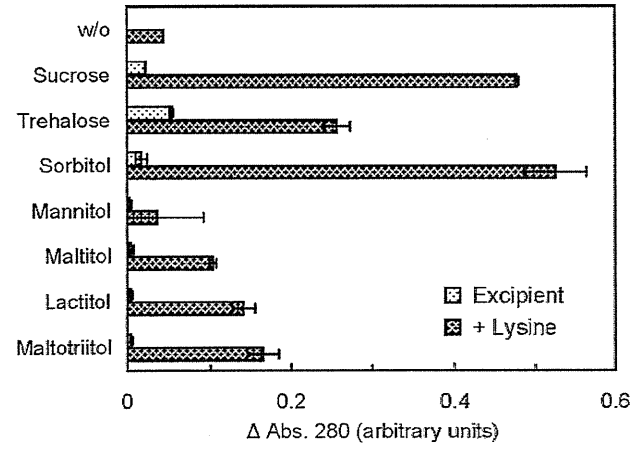

Fig. 5. Effect of storage (80 °C, 3 days) on non-enzymatic color development of solids freeze-dried from solutions containing L-lysine (5 mg/ml) and saccharides or sugar alcohols (100 mg/ml). Changes in the absorbance of re-hydrated solutions were obtained at 280 nm ($n = 3$).

compared to the non-reducing saccharides (sucrose, trehalose). Lower absorbance suggested limited reactivity of the partially crystallized mannitol in the dried solids.

4. Discussion

The results indicated the relevance of some oligosaccharide-derived sugar alcohols as principal stabilizers in the freeze-drying of proteins. An improved understanding the varied physical properties and protein-stabilizing mechanisms in the frozen solutions and freeze-dried solids, in comparison with those of disaccharides, will be indispensable for the rational application of the sugar alcohols.

The thermal transition and collapse onset temperatures (T_g', T_c) of frozen disaccharide-derived sugar alcohol solutions, comparable with those of structurally related saccharides, should allow freeze-drying by ordinary lyophilizers that are designed to cool their shelves down to −40 °C. Decreasing local viscosity of non-crystalline concentrated solute phases above the thermal transition (T_g') induces physical collapse from the drying interface (Pikal and Shah, 1990; Meister and Gieseler, 2009). The collapsed solids are not usually pharmaceutically acceptable because of their inelegant appearance and other changes in their physical properties (e.g., higher residual water, component crystallization) (Costantino et al., 1998). Controlling the shelf temperature to achieve a product slightly below T_g' or T_c (maximum allowable product temperatures) is usually recommended for efficient ice sublimation without collapse, since the ice sublimation speed increases significantly depending on the temperature (approx. 13% at 1 °C interval) (Pikal and Shah, 1990; Nail et al., 2002). Frozen saccharide solutions often show a T_c several degrees higher than the corresponding T_g', which difference depends on various factors, including the component composition and measurement methods (e.g., vacuum pressure, cell structure, type of microscope). Technical difficulties in distinguishing the changes at the collapse onset may partly explain the relatively large difference between the T_g' and T_c in the higher concentration (100 mg/ml) frozen excipient solutions.

The disaccharides and oligosaccharide-derived sugar alcohols formed cake-structure glass-state solids upon freeze-drying. Varied solid densities, degradation products, and residual water contents originating from the hydrated crystals may explain the different T_gs of some excipients prepared by freeze-drying and quench-cooling of the heat-melt. Addition of BSA and the buffer salts raised the transition temperature of the frozen solutions (T_g') and the dried solids (T_g) containing the oligosaccharide-derived sugar alcohols, suggesting their molecular-level mixing in the freeze-dried solid. Possible large molecular mobility during primary (low T_g' of frozen solutions) and/or secondary (low T_g of partially dried solids) drying processes should explain the partial crystallinity of glucose and sorbitol in the solids (Piedmonte et al., 2007).

The retention of the enzyme activity (LDH) and secondary structure (BSA) indicated that the oligosaccharide-derived sugar alcohols protected the proteins against stresses in each step of the freeze-drying process. LDH is a typical enzyme that irreversibly loses its activity by freeze-thawing and freeze-drying-induced subunit dissociation and conformation changes (Jaenicke, 1990; Anchordoquy et al., 2001; Bhatnagar et al., 2008). Various sugar alcohols (e.g., sorbitol, xylitol, maltitol) favor the native conformation of proteins over the unfolded states in the aqueous solutions in the same thermodynamic mechanism with those of saccharides (e.g., preferential exclusion) (Arakawa and Timasheff, 1982; Gekko, 1982; Gekko and Idota, 1989). In addition to the stabilization of aqueous proteins prior to freeze-drying and after rehydration, some sugar alcohols (e.g., xylitol, sorbitol) is considered to protect proteins from low-temperature-induced conformational changes in frozen solutions through the thermodynamic mechanism (Carpenter and Crowe, 1988; Arakawa et al., 2001). Sta-

bilization of proteins and cell membranes makes sorbitol a popular additive for food cryopreservation (e.g., minced fish meat) (Suzuki, 1981).

Extent of conformation changes by dehydration during secondary drying usually determines the lyophilization-induced protein inactivation (Jiang and Nail, 1998). The oligosaccharide-derived sugar alcohols (e.g., lactitol, maltitol) should substitute water molecules surrounding proteins that are essential to maintain the conformation during the freeze-drying process, as has been reported in oligosaccharides (Carpenter and Crowe, 1989). Insufficient number of water-substituting hydrogen bonds due to steric hindrance may explain the smaller structure-stabilizing effect of maltotriitol compared to maltitol and lactitol. Similar reductions of the structure-stabilizing effects have been reported in some larger oligosaccharides (e.g., maltotriose, maltotetraose, maltopentaose) and polysaccharides (e.g., dextran) (Tanaka et al., 1991; Izutsu et al., 2004). Crystallization during the freeze-drying process and storage deprives some sugar alcohols (e.g., mannitol, sorbitol) of the water-substituting molecular interaction (Izutsu et al., 1993; Cavatur et al., 2002; Piedmonte et al., 2007). Some non-crystallizing pentitols and hexitols (e.g., sorbitol) can provide additional protein-stabilizing water-substituting interactions in the co-lyophilization with some glass-forming or crystallizing excipients (Chang et al., 2005). Crystallization of mannitol in the frozen mixture solutions allows fast lyophilization that results in cake-structure microporous solids and dispersing amorphous regions containing proteins and protein-stabilizing excipients (e.g., sucrose) (Johnson et al., 2002).

The glass-state freeze-dried oligosaccharide-derived sugar alcohol solids should also protect embedded proteins from the chemical and physical degradation during storage. The high T_g and sufficient water-substituting interactions should make lactitol a preferable protein stabilizer over maltitol and maltotriitol for long-term storage of lyophilized solids (Hancock et al., 1995). The lower T_g amorphous solids are prone to faster chemical degradation and physical changes by the larger molecular mobility during storage and occasional exposure to temperatures above their T_g. Our present results also indicate the superior robustness of freeze-dried trehalose against the high-temperature stresses over the other saccharides and sugar alcohols studied. Co-lyophilization with some high T_g excipients (e.g., polymers) or excipients that intensify molecular interactions between stabilizing excipients (e.g., sodium phosphate) should be a potent method to raise the T_g of the amorphous sugar alcohol solids (Miller et al., 1998; Ohtake et al., 2004). The low enzyme activity remaining in the stored mannitol formulation suggested protection of the protein by rubber-state amorphous mannitol moiety dispersed in the physically stable crystalline cake.

In addition to the water-substitution and glass-embedding mechanisms, the oligosaccharide-derived sugar alcohols should protect protein structure in several other ways. They should dilute the non-ice phase in frozen solutions, and thus prevent protein denaturation by various stresses, including excess concentration of unfavorable co-solutes (e.g., inorganic salt), pH change by buffer opponent crystallization, and contact with ice surfaces. The sugar alcohols should also prevent crystallization of co-lyophilized saccharides (e.g., sucrose) during storage (Bhugra et al., 2007). The higher exclusion volume of larger sugar alcohol molecules (e.g., maltotriitol) should help to retain the integrity of the quaternary structure of LDH against the low-temperature-induced subunit dissociation that leads to irreversible structural change (Jaenicke, 1990; Anchordoquy et al., 2001).

The suggested lower susceptibility for the Maillard reaction should be an advantage to applying the oligosaccharide-derived sugar alcohols for freeze-drying of chemically labile proteins. The Maillard reaction, which often appears as non-enzymatic browning, is one of the major pathways of protein chemical degradation that also leads to biological activity loss (Manning et al., 1989; Kawai et al., 2004). The lower hydrolysis rate compared to some oligosaccharides should explain the limited reactivity of the sugar alcohols (Desai et al., 2007). Sucrose tends to be degraded into reactive reducing monosaccharides (glucose, fructose), as well as highly reactive fructofuranosyl cations during storage (Perez Locas and Yaylayan, 2008).

The oligosaccharide-derived sugar alcohols should be potent options in the formulation design as principal stabilizers that alternate disaccharides and/or an additional excipient to optimize the physical properties of the disaccharide-based formulations. Excipients appropriate for a particular therapeutic protein should vary depending on their chemical and physical stability, as well as their intended use. Further information on the safety and long-term protein stability would facilitate application of the oligosaccharide-derived sugar alcohols for freeze-dried protein formulations.

5. Conclusion

Some oligosaccharide-derived sugar alcohols (e.g., maltitol, lactitol, maltotriitol) formed glass-state amorphous cake-structure solids that protect model proteins from secondary structure perturbation (BSA) and activity loss (LDH) during freeze-drying and subsequent storage. Thermal and FDM analysis indicated applicability of ordinary lyophilizer for their freeze-drying without physical collapse during the process. The dried sugar alcohol solids have lower glass transition temperatures than the structurally related oligosaccharides, whereas lower susceptibility to Maillard reaction during storage should be an apparent advantage for particular applications.

Acknowledgements

This work was supported in part by the Japan Health Sciences Foundation (KHB1006).

References

Anchordoquy, T.J., Izutsu, K.I., Randolph, T.W., Carpenter, J.F., 2001. Maintenance of quaternary structure in the frozen state stabilizes lactate dehydrogenase during freeze-drying. Arch. Biochem. Biophys. 390, 35–41.

Arakawa, T., Prestrelski, S.J., Kenney, W.C., Carpenter, J.F., 2001. Factors affecting short-term and long-term stabilities of proteins. Adv. Drug Deliv. Rev. 46, 307–326.

Arakawa, T., Timasheff, S.N., 1982. Stabilization of protein structure by sugars. Biochemistry 21, 6536–6544.

Arakawa, T., Tsumoto, K., Kita, Y., Chang, B., Ejima, D., 2007. Biotechnology applications of amino acids in protein purification and formulations. Amino Acids 33, 587–605.

Bhatnagar, B.S., Pikal, M.J., Bogner, R.H., 2008. Study of the individual contributions of ice formation and freeze-concentration on isothermal stability of lactate dehydrogenase during freezing. J. Pharm. Sci. 97, 798–814.

Bhugra, C., Rambhatla, S., Bakri, A., Duddu, S.P., Miller, D.P., Pikal, M.J., Lechuga-Ballesteros, D., 2007. Prediction of the onset of crystallization of amorphous sucrose below the calorimetric glass transition temperature from correlations with mobility. J. Pharm. Sci. 96, 1258–1269.

Breen, E.D., Curley, J.G., Overcashier, D.E., Hsu, C.C., Shire, S.J., 2001. Effect of moisture on the stability of a lyophilized humanized monoclonal antibody formulation. Pharm. Res. 18, 1345–1353.

Carpenter, J.F., Crowe, J.H., 1988. The mechanism of cryoprotection of proteins by solutes. Cryobiology 25, 244–255.

Carpenter, J.F., Crowe, J.H., 1989. An infrared spectroscopic study of the interactions of carbohydrates with dried proteins. Biochemistry 28, 3916–3922.

Carrasquillo, K.G., Sanchez, C., Griebenow, K., 2000. Relationship between conformational stability and lyophilization-induced structural changes in chymotrypsin. Biotechnol. Appl. Biochem. 31, 41–53.

Cavatur, R.K., Vemuri, N.M., Pyne, A., Chrzan, Z., Toledo-Velasquez, D., Suryanarayanan, R., 2002. Crystallization behavior of mannitol in frozen aqueous solutions. Pharm. Res. 19, 894–900.

Chang, L.L., Shepherd, S., Sun, J., Tang, X.C., Pikal, M.J., 2005. Effect of sorbitol and residual moisture on the stability of lyophilized antibodies: implications for the mechanism of protein stabilization in the solid state. J. Pharm. Sci. 94, 1445–1455.

Costantino, H.R., 2004. Excipients for use in lyophilized pharmaceutical peptide, protein, and other bioproducts. In: Costantino, H.R., Pikal, M.J. (Eds.), Lyophiliza-

tion of Biopharmaceuticals. American Association of Pharmaceutical Scientsits, Arlington, pp. 139–228.
Costantino, H.R., Carrasquillo, K.G., Cordero, R.A., Mumenthaler, M., Hsu, C.C., Griebenow, K., 1998. Effect of excipients on the stability and structure of lyophilized recombinant human growth hormone. J. Pharm. Sci. 87, 1412–1420.
Desai, D., Rao, V., Guo, H., Li, D., Bolgar, M., 2007. Stability of low concentrations of guanine-based antivirals in sucrose or maltitol solutions. Int. J. Pharm. 342, 87–94.
Dong, A., Prestrelski, S.J., Allison, S.D., Carpenter, J.F., 1995. Infrared spectroscopic studies of lyophilization- and temperature-induced protein aggregation. J. Pharm. Sci. 84, 415–424.
Franks, F., 1992. Freeze-drying: from empiricism to predictability. The significance of glass transitions. Dev. Biol. Stand. 74, 9–18.
Gekko, K., 1982. Calorimetric study on thermal denaturation of lysozyme in polyol-water mixtures. J. Biochem. 91, 1197–1204.
Gekko, K., Idota, Y., 1989. Amino acid solubility and protein stability in aqueous maltitol solutions. Agric. Biol. Chem. 53, 89–95.
Griebenow, K., Klibanov, A.M., 1995. Lyophilization-induced reversible changes in the secondary structure of proteins. Proc. Natl. Acad. Sci. U.S.A. 92, 10969–10976.
Hancock, B.C., Shamblin, S.L., Zografi, G., 1995. Molecular mobility of amorphous pharmaceutical solids below their glass transition temperatures. Pharm. Res. 12, 799–806.
Hermeling, S., Crommelin, D.J., Schellekens, H., Jiskoot, W., 2004. Structure-immunogenicity relationships of therapeutic proteins. Pharm. Res. 21, 897–903.
Izutsu, K., Aoyagi, N., Kojima, S., 2004. Protection of protein secondary structure by saccharides of different molecular weights during freeze-drying. Chem. Pharm. Bull. 52, 199–203.
Izutsu, K., Kadoya, S., Yomota, C., Kawanishi, T., Yonemochi, E., Terada, K., 2009. Freeze-drying of proteins in glass solids formed by basic amino acids and dicarboxylic acids. Chem. Pharm. Bull. 57, 43–48.
Izutsu, K., Yoshioka, S., Terao, T., 1993. Decreased protein-stabilizing effects of cryoprotectants due to crystallization. Pharm. Res. 10, 1232–1237.
Izutsu, K., Yoshioka, S., Terao, T., 1994. Stabilizing effect of amphiphilic excipients on the freeze-thawing and freeze-drying of lactate dehydrogenase. Biotechnol. Bioeng. 43, 1102–1107.
Jaenicke, R., 1990. Protein structure and function at low-temperatures. Philos. Trans. R. Soc. Lond. B Biol. Sci. 326, 535–551.
Jiang, S., Nail, S.L., 1998. Effect of process conditions on recovery of protein activity after freezing and freeze-drying. Eur. J. Pharm. Biopharm. 45, 249–257.
Johnson, R.E., Kirchhoff, C.F., Gaud, H.T., 2002. Mannitol-sucrose mixtures–versatile formulations for protein lyophilization. J. Pharm. Sci. 91, 914–922.
Kawai, K., Hagiwara, T., Takai, R., Suzuki, T., 2004. Maillard reaction rate in various glassy matrices. Biosci. Biotechnol. Biochem. 68, 2285–2288.
Levine, H., Slade, L., 1988. Thermomechanical properties of small-carbohydrate-water glasses and rubbers. Kinetically metastable systems at sub-zero temperatures. J. Chem. Soc., Faraday Trans. 1 84, 2619–2633.
Liao, Y.H., Brown, M.B., Quader, A., Martin, G.P., 2002. Protective mechanism of stabilizing excipients against dehydration in the freeze-drying of proteins. Pharm. Res. 19, 1854–1861.
Manning, M.C., Patel, K., Borchardt, R.T., 1989. Stability of protein pharmaceuticals. Pharm. Res. 6, 903–918.
Meister, E., Gieseler, H., 2009. Freeze-dry microscopy of protein/sugar mixtures: Drying behavior, interpretation of collapse temperatures and a comparison to corresponding glass transition data. J. Pharm. Sci. 98, 3072–3087.
Miller, D.P., Anderson, R.E., de Pablo, J.J., 1998. Stabilization of lactate dehydrogenase following freeze-thawing and vacuum-drying in the presence of trehalose and borate. Pharm Res. 15, 1215–1221.
Nail, S.L., Jiang, S., Chongprasert, S., Knopp, S.A., 2002. Fundamentals of freeze-drying. Pharm. Biotechnol. 14, 281–360.
Ohtake, S., Schebor, C., Palecek, S.P., de Pablo, J.J., 2004. Effect of pH, counter ion, and phosphate concentration on the glass transition temperature of freeze-dried sugar-phosphate mixtures. Pharm. Res. 21, 1615–1621.
Perez Locas, C., Yaylayan, V.A., 2008. Isotope labeling studies on the formation of 5-(hydroxymethyl)-2-furaldehyde (HMF) from sucrose by pyrolysis-GC/MS. J. Agric. Food Chem. 56, 6717–6723.
Piedmonte, D.M., Summers, C., McAuley, A., Karamujic, L., Ratnaswamy, G., 2007. Sorbitol crystallization can lead to protein aggregation in frozen protein formulations. Pharm. Res. 24, 136–146.
Pikal, M.J., Shah, S., 1990. The collapse temperature in freeze-drying: dependence on measurement methodology and rate of water removal from the glassy phase. Int. J. Pharm. 62, 165–186.
Prestrelski, S.J., Tedeschi, N., Arakawa, T., Carpenter, J.F., 1993. Dehydration-induced conformational transitions in proteins and their inhibition by stabilizers. Biophys. J. 65, 661–671.
Shirke, S., Takhistov, P., Ludescher, R.D., 2005. Molecular mobility in amorphous maltose and maltitol from phosphorescence of erythrosin B. J. Phys. Chem. B 109, 16119–16126.
Slade, L., Levine, H., Ievolella, J., Wang, M., 2006. The glassy state phenomenon in applications for the food industry: application of the food polymer science approach to structure-function relationships of sucrose in cookie and cracker systems. J. Sci. Food Agric. 63, 133–176.
Suzuki, T., 1981. Fish and Krill Protein: Processing Technology. Applied Science Publishers, London.
Tamoto, K., Tanaka, S., Takeda, F., Fukumi, T., Nishiya, K., 1961. Studies on freezing of surimi and its application. IV. On the effect of sugar upon the keeping quality of frozen Alsaka pollock meat. Bull. Hokkaido Reg. Fish Res. Lab. 23, 50–60.
Tanaka, K., Takeda, T., Miyajima, K., 1991. Cryoprotection effect of saccharides on denaturation of catalase by freeze-drying. Chem. Pharm. Bull. 39, 1091–1094.
Tian, F., Middaugh, C.R., Offerdahl, T., Munson, E., Sane, S., Rytting, J.H., 2007. Spectroscopic evaluation of the stabilization of humanized monoclonal antibodies in amino acid formulations. Int. J. Pharm. 335, 20–31.
Wang, W., 2000. Lyophilization and development of solid protein pharmaceuticals. Int. J. Pharm. 203, 1–60.

Anal. Chem. **2010**, *82*, 7436–7443

Hyphenated Technique for Releasing and MALDI MS Analysis of O-Glycans in Mucin-Type Glycoprotein Samples

Keita Yamada,[†] Satomi Hyodo,[†] Mitsuhiro Kinoshita,[†] Takao Hayakawa,[‡] and Kazuaki Kakehi*[,†]

School of Pharmacy and Pharmaceutical Research and Technology, Kinki University

We developed an automatic apparatus for the release of O-glycans from mucin-type glycoproteins and proteoglycans (Matsuno, Y.-k.; Yamada, K.; Tanabe, A.; Kinoshita, M.; Maruyama, S.-z.; Osaka, Y.-s.; Masuko, T.; Kakehi, K. *Anal. Biochem.* 2007, *363*, 245–257. Yamada, K.; Hyodo, S.; Matsuno, Y. K.; Kinoshita, M.; Maruyama, S. Z.; Osaka, Y. S.; Casal, E.; Lee, Y. C.; Kakehi, K. *Anal. Biochem.* 2007, *371*, 52–61). The method allows rapid release of O-glycans as the reducing form within 10 min. In the present study, we connected the device to a MALDI-TOF MS spotter and achieved routine analysis of O-glycans in biological samples for clinical use after *in situ* derivatization of the released O-glycans with phenylhydrazine. We applied the method to the analysis of O-glycans expressed on MKN45 cells derived from human stomach cancer cells and found that MKN45 cells expressed characteristic trisialo-polylactosamine-type glycans as reported previously (Yamada, K.; Kinoshita, M.; Hayakawa, T.; Nakaya, S.; Kakehi, K. *J. Proteome Res.* 2009, *8*, 521–537). We also applied the method to the analysis of O-glycans in serum samples. The present technique is the first attempt to use MS measurement for routine clinical diagnostic works.

The O-linked glycans (O-glycans) in glycoproteins are covalently linked to Ser/Thr residues of the core protein through *N*-acetylgalactosamine (GalNAc) at their reducing ends. These glycans are often called as mucin-type glycans due to their predominant presence in tracheas and mucin secretory glands such as salivary glands. Currently, there are eight known core structures for O-glycans,[1] and a number of research works reported the aberrant glycan patterns in relation to the development and metastasis of malignancy.[2−4] Recently, Lebrilla and co-workers studied O-glycosylations in epithelial ovarian cancer cells and serum samples of breast cancer patients and proposed the use of O-glycans as clinical markers.[5,6]

Because various types of O-glycans are linked to the repeating Ser/Thr residues of Ser/Thr/Pro rich tandem repeating units of the core protein, direct analysis of the glycopeptides is difficult even if using the most newly developed analytical techniques such as mass spectrometry. Therefore, we have to release carbohydrate chains from the core proteins prior to the analysis. Various approaches to release glycans from the polypeptide backbone through the enzymatic or chemical procedures have been developed but have been a big challenge in the case of the analysis of O-glycans using a minute amount of glycoproteins.[1]

N-Glycanases (N-glycoamidases), the enzymes providing facile cleavage of asparagine-linked glycans (N-glycans), are revolutionary in the analysis of N-glycans.[7] In contrast, there is no enzyme which is capable of releasing a wide range of O-glycans from the core protein.[8] Therefore, we usually release O-glycans from the core proteins by chemical methods, typically by β-elimination with alkali in the presence of sodium borohydride or mild hydrazinolysis.[9,10]

N-Acetylgalactosamine (GalNAc) residues at the reducing end of mucin-type O-glycans are attached to Ser/Thr residues of mucin-type glycoproteins. To release the O-glycans, we usually use the alkali solution under mild conditions. However, if the GalNAc residues at the reducing end of the released glycans are substituted at the C-3 position, further degradation (i.e., peeling) tends to proceed. This is the most critical problem in the analysis of mucin-type O-glycans. Alkali-catalyzed β-elimination in the presence of sodium borohydride under mild conditions to prevent the "peeling" reaction is still the most common method for routine analysis of O-glycans,[11−13] and the method affords O-glycans as the reduced form (i.e., alditols). Consequently, the hemiacetal group at the reducing terminal is no longer available for chemical modification with fluorescent or UV-absorbing tags for their sensitive and high-resolution analysis. Royle and co-workers

* To whom correspondence should be addressed. Kowakae 3-4-1, Higashi-Osaka, 577-8502 Japan. Phone: +80-6-6721-2332. Fax: +80-6-6721-2353. E-mail: k_kakehi@phar.kindai.ac.jp.

[†] School of Pharmacy.

[‡] Pharmaceutical Research and Technology.

(1) Mechref, Y.; Novotny, M. V. *Chem. Rev.* **2002**, *102*, 321–369.
(2) Fuster, M. M.; Esko, J. D. *Nat. Rev. Cancer* **2005**, *5*, 526–542.
(3) Jensen, P. H.; Kolarich, D.; Packer, N. H. *FEBS J.* **2010**, *277*, 81–94.
(4) An, H. J.; Kronewitter, S. R.; De Leoz, M. L.; Lebrilla, C. B. *Curr. Opin. Chem. Biol.* **2009**, *13*, 601–607.
(5) Leiserowitz, G. S.; Lebrilla, C.; Miyamoto, S.; An, H. J.; Duong, H.; Kirmiz, C.; Li, B.; Liu, H.; Lam, K. S. *Int. J. Gynecol. Cancer* **2007**.
(6) Kirmiz, C.; Li, B.; An, H. J.; Clowers, B. H.; Chew, H. K.; Lam, K. S.; Ferrige, A.; Alecio, R.; Borowsky, A. D.; Sulaimon, S.; Lebrilla, C. B.; Miyamoto, S. *Mol. Cell. Proteomics* **2007**, *6*, 43–55.
(7) Takahashi, N. In *Handbook of Endoglycosidases and Glycoamidases*; Takahashi, N., Muramatsu, T., Eds.; CRC Press: Boca Raton, FL, 1992; p 183.
(8) Umemoto, J.; Bhavanandan, V. P.; Davidson, E. A. *J. Biol. Chem.* **1977**, *252*, 8609–8614.
(9) Merry, A. H.; Neville, D. C.; Royle, L.; Matthews, B.; Harvey, D. J.; Dwek, R. A.; Rudd, P. M. *Anal. Biochem.* **2002**, *304*, 91–99.
(10) Cancilla, M. T.; Penn, S. G.; Lebrilla, C. B. *Anal. Chem.* **1998**, *70*, 663–672.

10.1021/ac101581n
Published on Web 07/29/2010

employed mild hydrazinolysis to afford O-glycans from microgram quantities of glycoproteins, although a relatively lengthy time (~6 h) and the need for reacetylation of de-N-acetylated groups make it unsuitable for rapid analysis of multiple samples.[9] Karlsson and Packer reported an in-line flow releasing system employing alkaline β-elimination to release the reducing O-glycans from the core protein immobilized on the column, but this method also requires a long reaction time (16 h).[14] Huang et al. developed a method for releasing O-glycans in the presence of ammonia and successfully analyzed O-glycans from fetuin.[15] The method allowed simultaneous determination of both N- and O-glycans.

Recently, we developed an automatic O-glycan releasing apparatus for the release of O-glycans from mucin-type glycoproteins and proteoglycans and named the system "AutoGlycoCutter" (AGC).[16–19] Alkali-induced degradation of oligosaccharides (i.e., peeling reaction) has been a big problem during the alkali-catalyzed release of mucin-type glycans from the core peptides.[20] Use of the automatic device and optimization of experimental parameters dramatically improved the efficiency in the release of O-glycans in mucin-type glycoproteins. We successfully applied the device to the analysis of O-glycans from some leukemia and epithelial cancer cells and achieved identification of more than 80 O-glycans. Also, we found that polylactosamine-type O-glycans having larger molecular size than 6000 were present in a stomach cancer cell line (MKN 45 cells).[18] We suggested that these polylactosamine-type O-glycans might be a marker molecule of a stomach tumor.

However, to realize the O-glycan analysis in diagnostic works for the clinical purpose, we have to develop a full automatic machine from the releasing of O-glycans in biological samples to the analysis of glycan profiles. In the present study, we attempted hyphenation of the autoglycan releasing system with a sample spotter machine for the MALDI MS apparatus.

EXPERIMENTAL SECTION

Materials and Equipment. Bovine submaxillary mucin (BSM) was obtained from Sigma-Aldrich Japan (Shinagawa-ku, Tokyo, Japan). Phenylhydrazine and 2-aminobenzoic acid (2AA) for labeling of glycans were obtained from Tokyo Kasei Kogyo (Chuo-ku, Tokyo, Japan). 2,5-Dihydroxy benzoic acid (DHB) as the matrix material for MALDI MS measurement and Triton-X100 were also from Sigma-Aldrich Japan. Pronase (*Streptomyces griseus*) was obtained from Calbiochem (San Diego, CA). The protein inhibitor cocktail for animal cells was obtained from Nacarai Tesque (Nakagyo-ku, Kyoto, Japan). Ultrapure water by a Milli-Q water system (Millipore, Bedford, MA) was used. Other reagents and solvents were of the highest grade commercially available or HPLC grade.

MALDI-TOF MS spectra of O-glycans were acquired on a MALDI-QIT TOF mass spectrometer (AXIMA-QIT, Shimadzu, Kyoto, Japan). The instrument was operated in the positive-ion mode throughout the work, and acquisition and data processing were controlled by Launchpad software (Kratos Analytical, Manchester, U.K.). For collision-induced dissociation, argon gas was used as the collision gas.

Cell Culture. In the present study, we used MKN45 cells (human gastric adenocarcinoma cell line). The cells were cultured in RPMI-1640 medium supplemented with 10% (v/v) fetal calf serum and 1% (v/v) penicillin–streptomycin mixed solution (10 000 u penicillin and 10 mg of streptomycin/mL, Nacalai Tesque). Fetal calf serum was previously kept at 56 °C for 30 min. The cells were cultured at 37 °C under 5% CO_2 atmosphere and harvested at 80% confluent state. Collected cells (1×10^7 cells) were washed with phosphate buffered saline (PBS) and collected by centrifugation at 800*g* for 20 min.

Glycopeptide Pool from the Whole Cells. Cancer cells (2.0×10^7 cells) were suspended in 5 mM Tris-HCl buffer (pH 8.0, 500 μL) and mixed with an equal volume of 2% Triton X100 in the same buffer in an ice-bath. After homogenization of the cells for 7 min with a glass homogenizer, the mixture was centrifuged at 8000*g* for 30 min. The supernatant layer was collected and boiled for 7 min at 100 °C followed by evaporation to dryness by a centrifugal evaporator (SpeedVac, Savant, Sunnydale, CA). The lyophilized material was suspended in water (200 μL), and ethanol (800 μL) was added to the mixture to 80% concentration. The precipitate was collected by centrifugation and washed with ethanol (1 mL × 3) and then with acetone (1 mL × 2). The residue was dried in vacuo, and Pronase (50 μg) in 5 mM Tris-HCl (pH 8.0, 200 μL) was added, and the mixture was kept at 37 °C for 24 h. After the reaction mixture was boiled for 10 min, the supernatant was collected by centrifugation. Because cancer cells often contain a relatively large amount of free glycans in cytosols,[21] contaminated free glycans were previously reduced to the alditol form with sodium borohydride as follows: an aqueous solution of 2 M $NaBH_4$ (500 μL) was added to the supernatant and kept at room temperature for 30 min. Glacial acetic acid was carefully added to the mixture to decompose excess $NaBH_4$, and the mixture was passed through a centrifugal filter device (5 kDa cutoff). The solution was concentrated to 30 μL after washing with the water (400 μL × 3). A half of the solution (15 μL) was injected to the AGC-MS system.

Glycoprotein Pool from Serum Samples. A 50 μL portion of a human pooled serum sample (Wako Pure Chemicals) was diluted with water (200 μL), and the mixture was passed through a centrifugal filter device (10 kDa cutoff) to remove salts and low-molecular weight materials. The solution was concentrated to 30 μL after washing with water (250 μL × 3). Half of the solution (15 μL) was injected to the AGC-MS system.

(11) Kakehi, K.; Susami, A.; Taga, A.; Suzuki, S.; Honda, S. *J. Chromatogr., A* **1994**, *680*, 209–215.
(12) Schulz, B. L.; Packer, N. H.; Karlsson, N. G. *Anal. Chem.* **2002**, *74*, 6088–6097.
(13) Backstrom, M.; Thomsson, K. A.; Karlsson, H.; Hansson, G. C. *J. Proteome Res.* **2009**, *8*, 538–545.
(14) Karlsson, N. G.; Packer, N. H. *Anal. Biochem.* **2002**, *305*, 173–185.
(15) Huang, Y.; Mechref, Y.; Novotny, M. V. *Anal. Chem.* **2001**, *73*, 6063–6069.
(16) Matsuno, Y.-k.; Yamada, K.; Tanabe, A.; Kinoshita, M.; Maruyama, S.-z.; Osaka, Y.-s.; Masuko, T.; Kakehi, K. *Anal. Biochem.* **2007**, *362*, 245–257.
(17) Yamada, K.; Hyodo, S.; Matsuno, Y. K.; Kinoshita, M.; Maruyama, S. Z.; Osaka, Y. S.; Casal, E.; Lee, Y. C.; Kakehi, K. *Anal. Biochem.* **2007**, *371*, 52–61.
(18) Yamada, K.; Kinoshita, M.; Hayakawa, T.; Nakaya, S.; Kakehi, K. *J. Proteome Res.* **2009**, *8*, 521–537.
(19) Yamada, K.; Watanabe, S.; Kita, S.; Kinoshita, M.; Hayakawa, T.; Kakehi, K. *Anal. Biochem.* **2010**, *396*, 161–163.
(20) Lloyd, K. O.; Kabat, E. A.; Licerio, E. *Biochemistry* **1968**, *7*, 2976–2990.
(21) Ishiduka, A.; Hashimoto, Y.; Naka, R.; Kinoshita, M.; Kakehi, K.; Seino, J.; Funakoshi, Y.; Suzuki, T.; Kameyama, A.; Narimatsu, H. *Biochem. J.* **2008**.

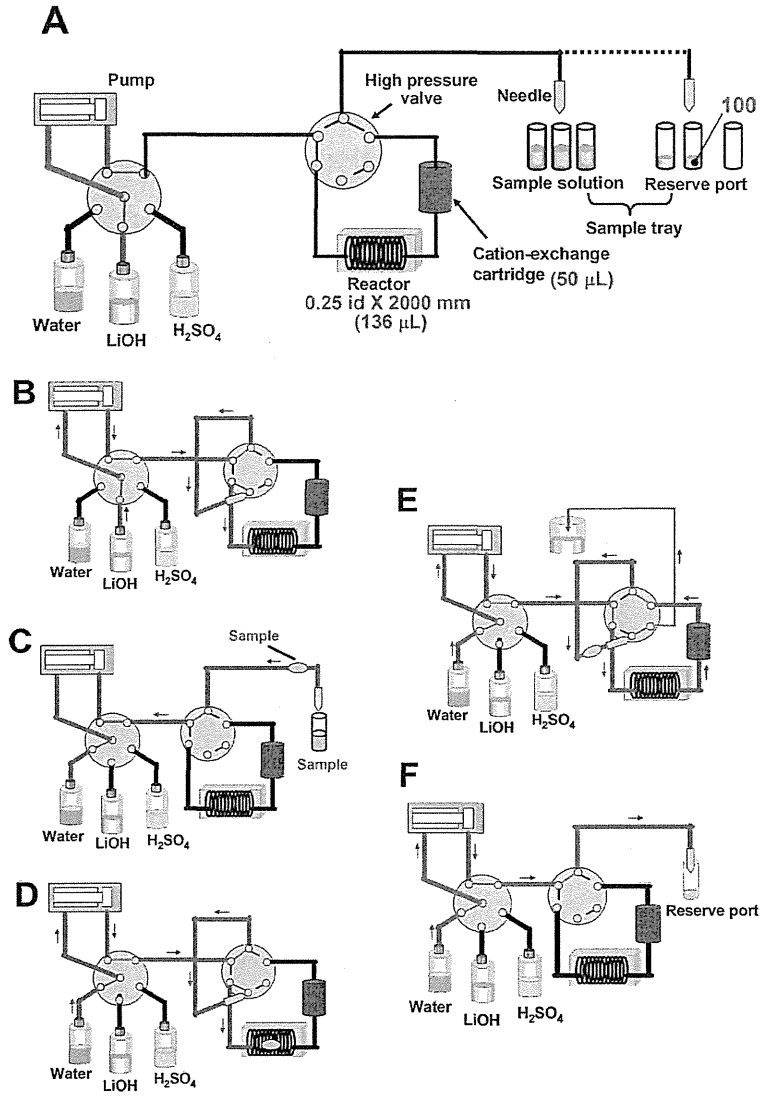

Figure 1. Flow diagram of the autoglycan releasing system.

Releasing Reaction of O-Glycans Using an AutoGlycoCutter System (AGC). The AGC system has been improved from the original version in order to be able to analyze microscale samples (Figure 1).[16] To release the O-glycans from glycoprotein samples, an aqueous solution (15 μL) of a glycoprotein sample was injected into the AGC. The AGC is composed of a pump, a reactor, a cartridge packed with cation exchange resin, a sample tray, and a switching valve (Figure 1A).

The glycan releasing reaction was performed as shown from parts B to F of Figure 1. When the program starts, the tubing of the reactor is filled with the alkali solution (0.5 M LiOH for glycan releasing) (Figure 1B). The introduced sample solution is mixed with the alkali solution and moved to the reactor at 120 μL/min (Figure 1C,D). When the mixed solution is introduced to the reactor, the flow is stopped and the solution is kept at the elevated temperature (45 °C) for a specified period (3.0 min). After the releasing reaction in the reactor, the mixture is pushed out from the reactor and passed through a small cartridge packed with cation-exchange resin (Figure 1E). The effluent from the cartridge is collected to the fraction collector (Figure 1F). In the present study, the effluent was divided and a portion (one tenth of the total volume) was introduced to the MALDI spotter (see below). The whole procedure was performed according to the automatic valve changing program and was completed within 4 min. After the run, the cation-exchange cartridge is regenerated with 0.25 M H_2SO_4. The collected solution (~100 μL) containing the released O-glycans were employed for the analysis by high-performance liquid chromatography and/or capillary electrophoresis after derivatization with a fluorescent labeling reagent such as 2-aminobenzoic acid (also see below).

Hyphenation of the AGC Apparatus to an Automatic Spotter Machine (AccuSpot) for MALDI MS Measurement: "AGC-MS System". A 10% portion of the reaction mixture was introduced to the MALDI plate as shown in Figure 2. An aqueous solution of 1.25% phenylhydrazine was mixed with the 10% flow of the eluate using a sheath flow device installed in the spotter machine at the rate of 1 μL/min. And the mixture was spotted onto the MALDI plate, on which a solution (1 μL) of 2,5-dihydroxybenzoic acid (10 mg/mL in 30% ethanol) had been previously spotted and air-dried at room temperature. The sampling rate was set at 20 s intervals. The solution on the MALDI plate is kept at 37 °C for 1 h, and MALDI MS spectra of O-glycans

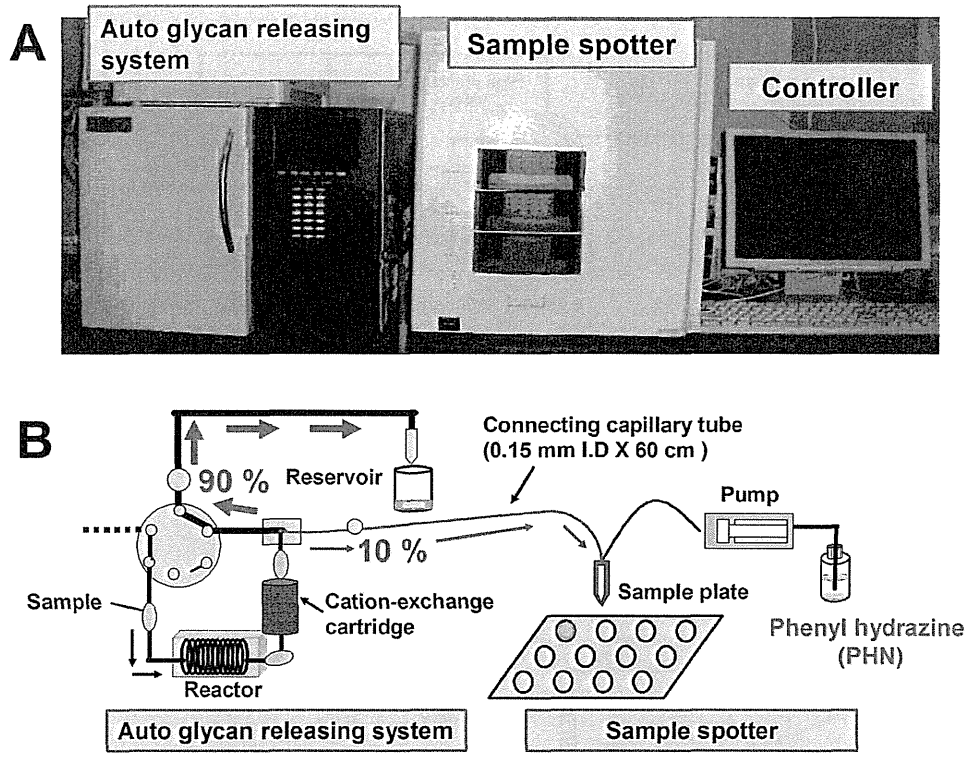

Figure 2. Auto glycan releasing system-MS system: (A) auto glycan releasing system-MS system. (B) Scheme for collection of the effluent from the Auto glycan releasing system. A 10% portion of the effluent is introduced to the spotter machine by adjusting the capillary size. In this case, we used a fused silica capillary (0.15 mm i.d., 60 cm). At the spotter port, an aqueous solution of 1.25% phenylhydrazine is mixed at the rate of 1 μL/min.

were acquired. The 90% portions of the eluate were recovered to the fraction collector and evaporated to dryness for further structural studies as well as quantitative analysis.

Fluorescent Labeling of the Released O-Glycans with 2-AA. The mixture of the released O-glycans in the 90%-portions of the eluate was dissolved in 2-AA solution (100 μL) freshly prepared by dissolution of 2-AA (30 mg) and sodium cyanoborohydride (30 mg) in methanol (1 mL) containing 4% sodium acetate and 2% boric acid. The mixture was kept at 80 °C for 1 h. Water (100 μL) was added after cooling, and the mixture was applied to a column of Sephadex LH-20 (1.0 cm i.d., 30 cm length) previously equilibrated with 50% aqueous methanol. The earlier eluted fluorescent fractions were pooled and evaporated to dryness under reduced pressure and used for the analysis by HPLC and CE.

CE Analysis of 2-AA Labeled O-Glycans. 2-AA-Labeled oligosaccharides were analyzed with a P/ACE MDQ glycoprotein system (Beckman Coulter, Fullerton, CA) equipped with a helium–cadmium laser-induced fluorescence detector (Ex 325 nm, Em 405 nm). Electrophoresis was performed using a DB-1 capillary (100 μm i.d., 30 cm length) in 100 mM Tris-borate buffer (pH 8.3) containing 5% polyethylene glycol (PEG70000) as the running buffer. Sample solutions were introduced into the capillary by pressure injection at 1 psi for 10 s. Separation was performed by applying the potential of 25 kV at 25 °C.

HPLC Analysis of 2-AA Labeled O-Glycans. The HPLC system was composed from a SCL-10A system controller (Shimadzu, Nakagyo-ku, Kyoto, Japan), two LC-10AD pumps (Shimadzu), a 655A-52 column oven (Hitachi, Chiyoda-ku, Tokyo, Japan), and an FP-920 fluorescence detector (JASCO, Hachi-oji, Tokyo, Japan) connected with a data processor (SmartChrom, KYA Technologies, Hachi-oji, Tokyo, Japan). Separation was done with a polymer-based Asahi Shodex NH2P-50 4E column (Showa Denko, Hachi-oji, Tokyo, Japan; 4.6 mm i.d., 250 mm length) using a linear gradient formed by 2% acetic acid in acetonitrile (solvent A) and 5% acetic acid in water containing 3% triethylamine (solvent B). The column was initially equilibrated and eluted with 70% solvent A for 2 min, then solvent B was increased to 95% over 80 min and kept at this composition for further 100 min. The flow rate was maintained at 1.0 mL/min through the analysis. Detection was performed by fluorometry at 350 nm for excitation and 425 nm for emission, respectively.

RESULTS AND DISCUSSION

Auto Glycan Releasing System (AutoGlycoCutter:AGC) for Online Analysis of O-Glycans in Mucin-Type Glycoproteins. Releasing of O-glycans attached to Ser/Thr residues of mucin-type glycoproteins has been a big problem in their analysis.[22] Recently, we developed an apparatus for the automatic release of O-glycans using an in-line flow system (AutoGlycoCutter-1, AGC-1).[16] The original version of the apparatus was designed for relatively large scale samples (~100 μg–1 mg), and a cartridge packed with cation exchange resin (1 mL) and a reactor of 700 μL volume were installed. To apply the method to the analysis of the smaller amount of samples with higher sensitivity, we miniaturized the system by using a cartridge of 50 μL volume packed with cation

(22) An, H. J.; Kronewitter, S. R.; de Leoz, M. L.; Lebrilla, C. B. *Curr. Opin. Chem. Biol.* **2009**, *13*, 601–607.

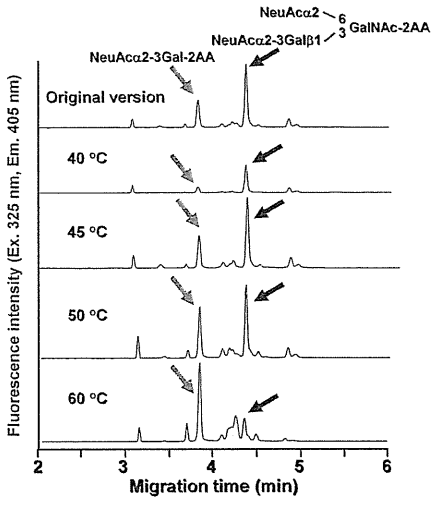

Figure 3. Optimization for oligosaccharide releasing reaction. O-Glycans released from the model glycopeptide by the automatic glycan-releasing system were analyzed by CE after labeling with 2-AA. The most upper panel shows the results on the analysis of O-glycans in the model glycopeptide using the original version of the auto glycan releasing system. The similar results were observed at 45 °C. Analytical conditions for CE: capillary, DB-1 capillary (100 m i.d., 30 cm); running buffer, 100 mM Tris-borate buffer (pH 8.3) containing 5% PEG70000; applied voltage, 25 kV; injection, pressure method (1 psi for 5 s); temperature, 25 °C; detection, helium–cadmium laser-induced fluorescence (excitation 325 nm, emission 405 nm).

exchange resin and a reactor having 136 μL volume. In addition, the dead volume was minimized by removing the detector. The volume (15 μL) of the sample solution was also fixed. In this device (Figure 1), the sample solution is brought to the reactor, then the flow is stopped for a specified time, and the releasing reaction occurs in the reactor. Then, the flow brings the sample zone to the cartridge (50 μL volume). It should be noted that these modifications minimizes diffusion of the sample zone, and the reaction mixture was recovered with the minimal dilution.

We optimized the conditions for glycan releasing reaction using a model glycopeptide derived from caseinoglycomacropeptide (cow milk) having the sequence GEPTSTPT.[17] Disialyl-T antigen, (NeuAcα2–3Galβ1-3(NeuAcα2-6)GalNAc, attaches to the fourth Thr residue (shown in bold face with underline) from the N-terminal. NeuAcα2-3Galβ1-3-residue of the disialyl T antigen is labile under alkaline conditions and forms degradation product (NeuAcα2-3Gal) by β-elimination (i.e., peeling reaction).[17,18] After the releasing reaction, the mixture of the released oligosaccharides was labeled with 2AA and analyzed by CE (Figure 3).

The disialyl-T and the degradation product (NeuAcα2-3Gal-2AA) were observed at 4.4 and 3.8 min, respectively. The best yield of disialyl-T was observed at 45 °C. At 40 °C, the yield of disialyl-T was lower than that at 45 °C. At the higher temperatures than 50 °C, the abundance of the peeling product (i.e., NeuAcα2-3Galβ1-3) became higher. The yield of the disialyl T from the model peptide obtained under the optimized conditions (reaction solution, 0.5 M LiOH; reaction time, 3 min; reaction temperature, 45 °C) was 58.8 ± 3% (n = 5) when determined by CE. The ratio of the degradation product was 24.4 ± 1%. It should be noted that the present method showed excellent repeatability, although partial degradation was observed.

Hyphenation of AGC with a Spotter Machine for MALDI MS Measurement. We directly connected the auto glycan releasing system to the spotter machine for MALDI MS measurement (Figure 2). The effluent from the cartridge was divided by a splitter, and a 10% portion of the effluent was introduced to the MALDI spotter. By adjusting the length and the internal diameter of tubing (0.15 mm i.d., 60 cm length), we could introduce one tenth of the sample solution to the MALDI plate and the effluent was automatically mixed with an aqueous solution of the matrix (DHB). However, we could not detect the molecular ions due to free O-glycans released from the core peptides with high sensitivity (data not shown). This is probably due to the presence of contaminated peptide fragments and other materials during the releasing reaction.

To improve the sensitivity in detection of the glycans, on-plate derivatization of O-glycans in the effluent collected on the MALDI plate was examined. Lattova et al. reported that phenylhydrazine was a useful derivatization reagent for highly sensitive detection of glycans in clinical samples. The method is based on on-plate derivatization of glycans with phenylhydrazine to form phenylhydrazone. The phenylhydrazone thus formed on the plate was detected by a MALDI-MS apparatus.[23,24] In the present study, we introduced a 1.25% aqueous solution of phenylhydrazine to be mixed with the effluent from AGC, and the mixture was spotted onto the plate, on which DHB solution had been previously spotted and dried. The mixture on the target was kept at 37 °C for 1 h to complete the derivatization reaction according to the method reported by Lattova et al.[23,24] We can use a diluted phenylhydrazine solution due to its high reaction efficiency in hydrazone formation. In addition, because the effluent was passed through a cartridge packed with cation exchange resin, it showed acidic property which is preferable for hydrazone formation. It should be noticed that phenylhydrazone derivatives of reducing carbohydrates are easily crystallizable and may be a strong point for MALDI MS measurement. In addition, it was not necessary to

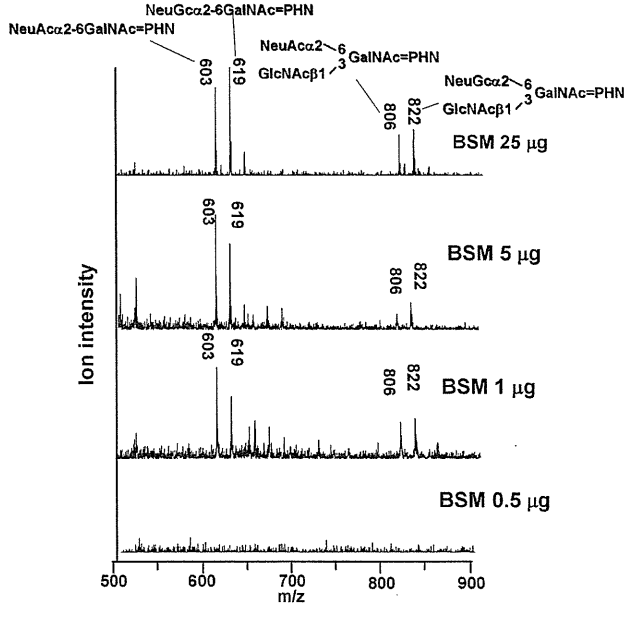

Figure 4. Detection limit of the autoglycan releasing system-MS system as examined using bovine submaxillary mucin as a model sample.

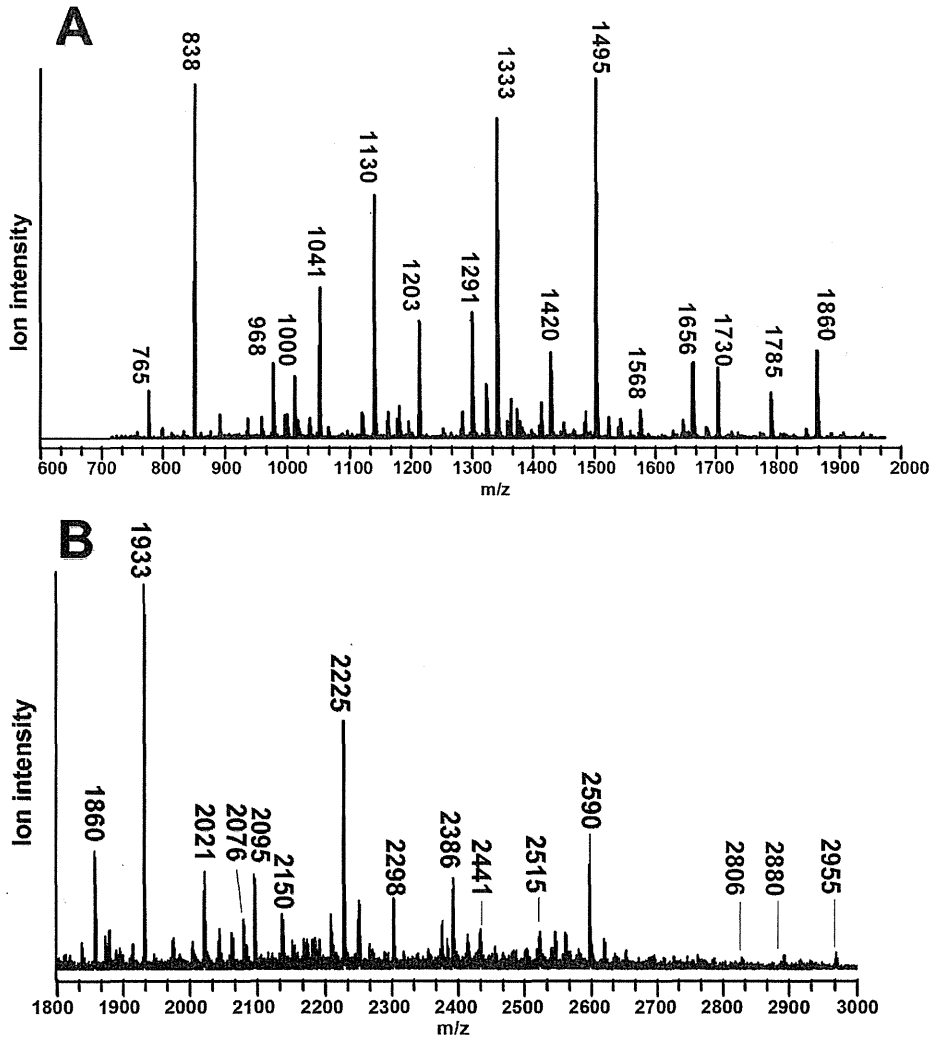

Figure 5. Analysis of O-glycans from MKN45 cells. The results for the low- and high-mass ranges are shown in parts A and B, respectively.

remove the excess phenylhydrazine by washing. Thus, the whole procedure from the releasing of O-glycans to MS measurement was completed within 1.5 h.

On the basis of the studies described above, we applied the present technique to the analysis of O-glycans from bovine submaxillary mucin (BSM). The results are shown in Figure 4.

When using 25 μg of BSM (2.5 μg as the injected amount), we could easily observe the major molecular ions due to O-glycans. Two molecular ions observed at m/z 603 and m/z 619 are due to NeuAcα2-6GalNAc=PHN and NeuGcα2-6GalNAc=PHN, respectively. Two molecular ions observed at m/z 806 and 822 are confirmed as sialyl-core 3 structures, GlcNAcβ1-3(NeuAcα2−6) GalNAc=PHN and GlcNAcβ1-3(NeuGcα2-6) GalNAc=PHN, respectively. Sialic acids of O-glycans in BSM have two forms of *N*-acetyl neuraminic acid and *N*-glycolyl neuraminic acid. Therefore, we could observe two sets of the molecular ions of O-glycans.[11] Even at the 1 μg-level of the sample (0.1 μg as the amount injected to the MALDI plate), we clearly observed the molecular ions of these glycans.

(23) Lattova, E.; Chen, V. C.; Varma, S.; Bezabeh, T.; Perreault, H. *Rapid Commun. Mass Spectrom.* **2007**, *21*, 1644–1650.
(24) Lattova, E.; Kapkova, P.; Krokhin, O.; Perreault, H. *Anal. Chem.* **2006**, *78*, 2977–2984.

Application to the Analysis of O-Glycans Derived from Cancer Cells. We applied the present method to the analysis of O-glycans expressed on MKN45 cells (a human stomach cancer cell line). O-Glycans of glycopeptide fractions obtained from the whole cells after digestion with Pronase were analyzed by the present method. The results observed for low- and high-molecular ranges are shown in parts A and B of Figure 5, respectively, and the list of the proposed structures based on our previously reported data is summarized in Table 1.[18]

Two molecular ion peaks observed at m/z 838 and m/z 1041 are due to asialo core 2 type structures, Galβ1-3(Galβ1-4GlcNAcβ1-6)-GalNAc=PHN and Galβ 1-3(GlcNAcβ- Galβ1-4GlcNAcβ1-6)-GalNAc=PHN, respectively. Four molecular ion peaks at m/z 1203, 1568, 1933, and 2298 are confirmed as asialo polylactosamine-type O-glycans, Galβ1-3((Galβ-GlcNAcβ)$_n$-Galβ1-4-GlcNAcβ1-6) GalNAc=PHN (n = 1−4). The molecular ion peak observed at m/z 765 corresponds to sialyl-T, NeuAcα2-3Galβ1-3GalNAc=PHN. Three molecular ion peaks observed at m/z 968, 1130, and 1333 are assigned as monosialo core 2 type glycans, Galβ1-3(GlcNAcβ1-6)GalNAc=PHN + NeuAc$_1$, Galβ1-3(Galβ1-4GlcNAcβ1-6) GalNAc=PHN + NeuAc$_1$, and Galβ1-3(GlcNAcβ-Galβ1-4GlcNAcβ1-6)GalNAc=PHN + NeuAc$_1$, re-

Table 1. O-Glycans Observed in MKN45 Cells

proposed structures	observed molecular mass (m/z)
Asialo Glycans	
Galβ1-3(Galβ1-4GlcNAcβ1-6)GalNAc=PHN	838
Galβ1-3(GlcNAc-Galβ1-4GlcNAcβ1-6)GalNAc=PHN	1041
Galβ1-3(Gal-GlcNAc-Galβ1-4GlcNAcβ1-6)GalNAc=PHN	1203
Galβ1-3((Gal-GlcNAc)$_2$-Galβ1-4GlcNAcβ1-6)GalNAc=PHN	1568
Galβ1-3((Gal-GlcNAc)$_3$-Galβ1-4GlcNAcβ1-6)GalNAc=PHN	1933
Galβ1-3((Gal-GlcNAc)$_4$-Galβ1-4GlcNAcβ1-6)GalNAc=PHN	2298
Monosilao Glycans	
NeuAcα2-3Galβ1-3GalNAc=PHN	765
Galβ1-3(GlcNAcβ1-6)GalNAc=PHN + NeuAc$_1$	968
Galβ1-3(Galβ1-4GlcNAcβ1-6)GalNAc=PHN + NeuAc$_1$	1130
Galβ1-3(GlcNAc-Galβ1-4GlcNAcβ1-6)GalNAc=PHN + NeuAc$_1$	1333
Galβ1-3(Gal-GlcNAc-Galβ1-4GlcNAcβ1-6)GalNAc=PHN + NeuAc$_1$	1495
Galβ1-3((Gal-GlcNAc)$_2$-Galβ1-4GlcNAcβ1-6)GalNAc=PHN + NeuAc$_1$	1860
Galβ1-3((Gal-GlcNAc)$_3$-Galβ1-4GlcNAcβ1-6)GalNAc=PHN + NeuAc	2225
Galβ1-3((Gal-GlcNAc)$_4$-Galβ1-4GlcNAcβ1-6)GalNAc=PHN + NeuAc	2590
Galβ1-3((Gal-GlcNAc)$_5$-Galβ1-4GlcNAcβ1-6)GalNAc=PHN + NeuAc	2955
Disialo Glycans	
NeuAc-Galβ1-3(NeuAc-Galβ1-4GlcNAcβ1-6)GalNAc=PHN	1420
NeuAc-Galβ1-3(NeuAc-Gal-GlcNAc-Galβ1-4GlcNAcβ1-6)GalNAc=PHN	1785
NeuAc-Galβ1-3(NeuAc-(Gal-GlcNAc)$_2$-Galβ1-4GlcNAcβ1-6)GalNAc=PHN	2150
NeuAc-Galβ1-3(NeuAc-(Gal-GlcNAc)$_3$-Galβ1-4GlcNAcβ1-6)GalNAc=PHN	2515
NeuAc-Galβ1-3(NeuAc-(Gal-GlcNAc)$_4$-Galβ1-4GlcNAcβ1-6)GalNAc=PHN	2880
Trisialo Glycans	
NeuAc-Gal-GlcNAc-(NeuAc-Gal-GlcNAc)Galβ1-3(NeuAcα2-6)GalNAc=PHN	2076
NeuAc-Gal-GlcNAc-(NeuAc-Gal-GlcNAc)Galβ1-3(NeuAcα2-6)GalNAc=PHN + Gal-GlcNAc	2441
NeuAc-Gal-GlcNAc-(NeuAc-Gal-GlcNAc)Galβ1-3(NeuAcα2-6)GalNAc=PHN + (Gal-GlcNAc)$_2$	2806
Degradation Product	
(Gal-GlcNAc)$_2$-Gal=PHN	1000
NeuAc-(Gal-GlcNAc)$_2$-Gal=PHN	1291
NeuAc-(Gal-GlcNAc)$_3$-Gal=PHN	1656
(Gal-GlcNAc)$_4$-Gal=PHN	1730
NeuAc-(Gal-GlcNAc)$_4$-Gal=PHN	2021
(Gal-GlcNAc)$_5$-Gal=PHN	2095
NeuAc-(Gal-GlcNAc)$_5$-Gal=PHN	2386

spectively. Five molecular ion peaks at m/z 1495, 1860, 2225, 2590, and 2955 are due to monosialo polylactosamine-type O-glycans, Galβ1-3((Galβ-GlcNAcβ)$_n$-Galβ1-4GlcNAcβ1-6)GalNAc=PHN + NeuAc$_1$ (n = 1−5). Disialo polylactosamine-type O-glycans were also observed in MKN45 cells. Four molecular ion peaks at m/z 1785, 2150, 2515, and 2880 are confirmed as disialo core 2 type glycans modified with 1−7 units of lactosamine residues. Three molecular ion peaks containing three sialic acid residues were observed at m/z 2076, 2441, and 2806 are due to NeuAc$_3$Hex$_3$HexNAc$_3$=PNH, NeuAc$_3$Hex$_4$HexNAc$_4$=PNH, and NeuAc$_3$Hex$_5$HexNAc$_5$=PNH, respectively. As reported previously, these trisialo glycans are core 1 type glycans having the structures as indicated below.[18]

NeuAcα(Galβ1-4GlcNAcβ)nNeuAcα2-6GalNAc
NeuAcα(Galβ1-4GlcNAcβ)mGalβ1-3

These structures were observed exclusively in MKN45 cells according to our recent research results, and we suggested that these O-glycans might be a specific marker of gastric adenocarcinoma.[18] Seven molecular ion peaks observed at m/z 1000, 1291, 1656, 1730, 2021, 2095, and 2386 are due to the degradation products from these trisialo core 1 type polylactosamine glycans, NeuAc-(Galβ-GlcNAcβ)$_n$-Gal=PHN (n = 1−5), and the presence of these products means that these glycans occupy the 1-3 linked arm of the glycans because of easy degradation (i.e., peeling). Therefore, these glycans are important keys for structural confirmation of the parent glycans.[18]

Analysis of O-Glycans Derived from Serum Glycoproteins Using AGC-MS System. Another application to the analysis of O-glycans in a serum sample is shown in Figure 6. After brief deionization of the diluted solution using an ultramembrane filter, the solution was easily analyzed by the present system. As indicated in Figure 6A, several molecular ions were observed. The molecular ion peaks observed at m/z 765 with sodium adduct ion (m/z 787) are confirmed as sialyl-T.

The molecular ion peak observed at m/z 1056 corresponds to disialyl-T. The molecular ion peaks observed at m/z 562 with sodium adduct ion m/z 584 are due to a peeling product (NeuAc α2-3Gal=PNH). After the releasing reaction is performed in the flow of an aqueous LiOH solution, the reaction mixture is passed through a cartridge packed with cation exchange resin. Therefore, the effluent from the device does not contain cation(s) as examined by the absence of Li adduct ion in the MS spectra. Then, the effluent from the device is mixed with diluted phenylhydrazine solution and spotted onto the MALDI plate. Accordingly, the phenylhydrazone on the MALDI plate theoretically only shows protonated ions. In this case, however, diluted phenylhydrazine solution probably contains a trace amount of sodium ion, and the MS gives sodium adduct ions as well as protonated ions.

To confirm these peaks, we also analyzed the O-glycans obtained from the split effluent (collected by the fraction collector)

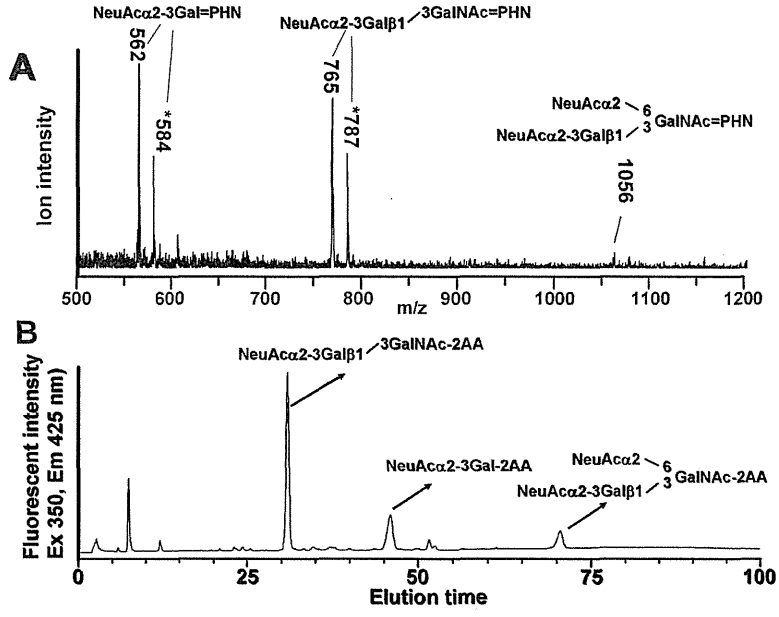

Figure 6. Analysis of O-glycans in a pooled serum sample. (A) MS analysis of the O-glycans by the present method. (B) Analysis of the O-glycans in a pooled serum sample by HPLC. The nine tenth portions of the O-glycans released by the autoglycan releasing system-MS system were labeled with 2-AA and analyzed by HPLC. Analytical conditions for HPLC: column, Asahi Shodex NH2P-50 4E (4.6 mm × 250 mm); eluent, solvent A, 2% CH_3COOH in acetonitrile; solvent B, 5% CH_3COOH/3% triethylamine in water, gradient condition, linear gradient (30–95% solvent B) from 2 to 82 min, maintained for 20 min.

as 2-AA derivatives using HPLC (Figure 6B). Each of the peaks was collected and compared with the standard samples by MALDI-TOF MS as reported previously.[18] The most abundant peak observed at 31 min is due to sialyl-T which shows the molecular ion at *m/z* 765. The peak observed at 71 min is derived from disialyl-T which shows the molecular ion at *m/z* 1085. We also observed the peak due to the peeling product (NeuAcα2-3Gal-2AA) at 45 min. These results were in good agreement with the direct MS analysis as shown in Figure 6A, although the relative abundances of these glycans are different between HPLC and MS methods. The HPLC/CE-fluorescent detection method affords accurate amounts of the glycans based on the fluorescent intensity of the 2-aminobenzoic acid residue at the reducing terminal. A combination of both methods will be a powerful tool for accurate diagnosis of the disease or disease states.

CONCLUSIONS

We have been developing an automatic device for releasing O-glycans from the mucin-type glycoproteins.[17–19] In the present paper, we connected the device to a spotter machine for MALDI MS measurement and attempted direct measurement of O-glycans. Because we could not observe the molecular ions of free glycans by direct measurement due to their low sensitivity and the presence of contaminated materials during releasing reactions, we labeled the released O-glycans with phenylhydrazine by *in situ* derivatization to achieve highly sensitive detection of O-glycans by MS measurement. The derivatization reaction proceeded under mild conditions even in the presence of 2,5-dihydroxybenzoic acid (matrix material). Accordingly, we performed the analysis from the glycan releasing reaction to MS measurement within 1.5 h.

The system allows MS analysis of O-glycans of bovine submaxillary mucin even when using 1 μg of the protein sample (actual sample amount 100 ng). We applied the present technique to the analysis of the O-glycans expressed on MKN45 cells derived from human stomach adenocarcinoma and found that trisialo-O-glycans were present abundantly as reported previously.[18] In addition, O-glycans in a pooled serum sample were also successfully analyzed. It is well-known that quantitative analysis is often difficult in MS measurement. Fluorescence detection by HPLC/CE gives robust and reproducible results in quantitative analysis. The data in Figure 6 indicate that the proposed method using the hyphenated glycan-releasing and MS analysis shows similar glycan profiles with those obtained by HPLC, but the relative abundances of the glycans are somewhat different from those observed by HPLC/CE analysis. However, extremely high-throughput characteristics of the present method will be quite important in routine analysis of glycans for clinical use. We believe that the present technique is the primary attempt to use MS measurement for routine clinical diagnostic works.

Received for review June 15, 2010. Accepted July 20, 2010.

AC101581N

Research Article

Biomedical Chromatography

Received 16 April 2010, Revised 3 June 2010, Accepted 4 June 2010 Published online in Wiley InterScience

(www.interscience.wiley.com) DOI 10.1002/bmc.1486

Determination of sulfate ester content in sulfated oligo- and poly-saccharides by capillary electrophoresis with indirect UV detection

Mitsuhiro Kinoshita[a], Naotaka Kakoi[a], Yu-ki Matsuno[b], Takao Hayakawa[c] and Kazuaki Kakehi[a]*

ABSTRACT: Carbohydrates having sulfate groups such as glycosaminoglycans and chemically synthesized sucrose sulfate show interesting and important biological activities. We adapted CE with indirect UV detection technique to the determination of sulfate ester in sulfated carbohydrates, which were previously hydrolyzed with HCl. The liberated sulfate ion was analyzed using a background electrolyte consisting of triethanolamine-buffered chromate with hexamethonium bromide. Sulfate contents of glucose 3-sulfate and sucrose octasulfate used as a model were in good agreement with theoretical values (accuracy, 95.9–96.7 and 97.4–101.9%, respectively), and relative standard deviation values run-to-run were 0.977 and 1.90%, respectively. We applied the method to the determination of the sulfate contents of some glycosaminoglycan samples and showed that the contents were in good agreement with those calculated from sulfur content. Copyright © 2010 John Wiley & Sons, Ltd.

Keywords: sulfate; glycosaminoglycans; capillary electrophoresis indirect UV detection

Introduction

Sulfation of hydroxyl and amino groups (-O-SO_3H and -NH-SO_3H) is one of the common modifications of carbohydrates and is often observed in various glycoconjugates such as proteoglycans or mucin-like glycoproteins. Sulfated carbohydrates are widely distributed in animals as the major constituents of proteoglycans and are biologically active molecules involved in various biological events (Hooper *et al.*, 1996; Honke and Taniguchi, 2002; Wu, 2006). Functions of sulfated carbohydrates strongly depend on the presence and spatial positioning in the molecules. Degree of sulfation on carbohydrates is also closely related to biological activities such as blood coagulation, signal transduction and cell–cell interaction (Lindahl *et al.*, 1983; Villanueva, 1984; Hemmerich and Rosen, 1994; Small *et al.*, 1996; Tsuboi *et al.*, 1996). Chemical sulfation of carbohydrates often affords compounds showing novel biological activities such as anti-HIV activities (Katsuraya *et al.*, 1994, 1999; Yoshida *et al.*, 1995; Hattori *et al.*, 1998). Sulfated carbohydrates also have potential as pharmaceuticals (Werz and Seeberger, 2005). Sucrose octasulfate, 'Sucralfate' and the chemically synthesized octasulfated pentasaccharide 'Arixtra' are used as antiulcer and anticoagulant drugs, respectively (Candelli *et al.*, 2000; Giangrande, 2002).

In view of these interesting features of sulfated carbohydrates, assessment of sulfate content is important not only for the understanding of their biological significance but also the development and manufacturing of novel bioactive sulfated carbohydrates. Several methods have been developed for the determination of sulfate content of carbohydrates. Classical methods are based on the colorimetric determination of the inorganic sulfate ion liberated from sulfated carbohydrates by acid hydrolysis, such as chelating barium ions with rhodizonate (Terho and Hartiala, 1971; Roy and Turner, 1982). Srinivasan *et al.* achieved the determination of microgram quantity of sulfate ion based on the formation of stable complex of sulfate ester with *n*-butylamine and achieved determination of microgram quantity of sulfate ion (Srinivasan *et al.*, 1970). Unfortunately, these methods are not suitable for the determination of a small amount of sulfate ester in complex carbohydrate, because they are time-consuming and not sensitive enough, require a significant amount of material, and are prone to interference from the other ions. Compared with these conventional methods, ion chromatography (IC) demonstrates increased specificity and sensitivity

* Correspondence to: K. Kakehi, Faculty of Pharmaceutical Sciences, Kinki University, Kowakae 3-4-1, Higashi-osaka 577-8502, Japan. E-mail: k_kakehi@phar.kindai.ac.jp

[a] Faculty of Pharmaceutical Sciences, Kinki University, Kowakae 3-4-1, Higashi-osaka 577-8502, Japan

[b] Research Center for Medical Glycoscience, National Institute of Advanced Industrial Science and Technology, Open Space Laboratory C-2, 1-1-1 Umezono, Tsukuba, Ibaraki 305-8568, Japan

[c] Pharmaceutical Research and Technology Institute, Kinki University, Kowakae 3-4-1, Higashi-osaka 577-8502, Japan

Abbreviations used: BGE, background electrolyte; CSA, chondroitin sulfate A; DMF, *N,N*-dimethylformamide; DS, dermatan sulfate; GAG, glycosaminoglycan; HA, hyaluronic acid; HMB, hexamethonium bromide; HP, heparin; HS, heparan sulfate; TBA, tributylamine; TEA, triethanolamine.

as well as the inherent ability for the determination of various inorganic ions, and has been applied to the analysis of the ions in the samples from biological, environmental and industrial origins (Lopez-Ruiz, 2000). The sulfate contents in glycoproteins or GAGs were successfully determined by IC (Cole and Evrovski, 1997; Toida *et al.*, 1999). Toida *et al.* liberated the sulfate ion from chemically O-sulfated GAGs by acid hydrolysis, and determined it by a combination of IC and conductivity detection (Tadano-Aritomi *et al.*, 2001).

Capillary electrophoresis (CE) is a powerful tool for separation of inorganic ions with high resolving power. Its performance is comparable with that of IC, and has become one of the standard tools for the analysis of inorganic ions in environmental, biomedical, clinical and industrial samples (Fritz, 2000; Timerbaev, 2002, 2004; Johns *et al.*, 2003; Pacakova *et al.*, 2003; Paull and King, 2003). CE allows rapid analysis with high resolution and exhibits good capabilities in quantitative analysis, making it well suited for routine analysis of sulfate content of carbohydrates. Although the detection in CE is usually performed by direct UV detection, most inorganic ions lack a chromophore and cannot be detected using common direct UV detection. Therefore, indirect UV detection technique is usually used for determination of inorganic ions. Indirect UV detection adds an UV-absorbing co-ion (called the probe) to the background electrolyte (BGE) and this probe is displaced by migration, causing a negative signal. Indirect UV detection is an effective alternative detection technique for inorganic ions. The attractive performance of the CE method has been employed for the assay of sulfotransferase activity (Saillard *et al.*, 1999). Thus, CE is considered a useful alternative to the well-established IC method for routine analysis of sulfate content of carbohydrates.

In the present study, we developed a method using capillary electrophoresis with indirect UV detection to the determination of sulfate content of sulfated oligo-/polysaccharides, and applied the method for the determination of sulfate content in some sulfated GAGs and the monitoring of chemically sulfation reaction of polysaccharides. The present method will provide a robust method for the analysis of sulfated carbohydrates using routinely available laboratory instrumentation.

Experimental

Materials

Hexamethonium bromide, glucose 3-sulfate (sodium salt, 98% purity by HPLC), sucrose octasulfate (sodium salt) and heparin from bovine intestinal mucosa were purchased from Sigma (St Louis, MO, USA). Hyaluronic acid (from *Streptococcus zooepidemicus*) was purchased from Nacalai tesque (Uji, Kyoto, Japan). Chondroitin sulfate A (from whale cartilage), dermatan sulfate (from pig skin) and heparan sulfate (from bovine kidney) were purchased from Seikagaku Biobusiness (Chiyoda-ku, Tokyo, Japan). Tributylamine (TBA), *N,N*-dimethylformamide (DMF) and pyridine–sulfur trioxide complex were obtained from Wako Pure Chemicals (Dosho-machi, Osaka, Japan). All other chemicals and reagents were of the highest grade or HPLC grade. Running buffers and aqueous solutions were prepared with water purified with a Milli-Q purification system (Millipore, Bedford, MS, USA).

Sulfation of Chondroitin Sulfate A

Chemical sulfation of chondroitin sulfate A was performed according to the method reported by Maruyama *et al.* (1998). The sodium salt (10 mg) of chondroitin sulfate A (from whale cartilage) was dissolved in 1 mL of 5% TBA–HCl water (pH 2.8), and then the solution was lyophilized to dryness to give the tributylammonium salt. The salt was dissolved in 1 mL of DMF, and pyridine–sulfur trioxide complex (10, 50, 100 and 250 mg) was added. After incubating the mixture for 1 h at 40°C, the reaction was terminated by addition of water (1 mL). The reaction product was precipitated with cold ethanol (6 mL) saturated with anhydrous sodium acetate, collected by centrifugation at 4°C, then dissolved in water followed by dialysis against water to remove salts and lyophilized. We obtained $PSCS_{10}$ (11.8 mg), $PSCS_{50}$ (14.1 mg), $PSCS_{100}$ (17.2 mg) and $PSCS_{250}$ (18.6 mg), respectively, by changing the amount of pyridine–sulfur trioxide complex.

Sample and Standard Solutions

Standard solutions of sulfate ion were prepared by dissolving an accurately weighed amount of sodium sulfate (300 mg) in water (10 mL; 210 mM). A series of standard solutions of sulfate ion for calibration curve were prepared by appropriate dilution of the standard solution with water. Sample solution of sulfated oligo-/polysaccharides was also prepared by dissolving an accurately weighed amount (1.00 mg) in of water (1 mL).

CE Analysis of Sulfate Ion with Indirect UV Detection

CE was performed with a Beckman P/ACE MDQ system equipped with a UV detector (Beckman Coulter, Fullerton, CA, USA). A fused silica capillary (50 μm i.d., 56 cm effective length, 66 cm total length, from Agilent Technologies) was used throughout the work. The background electrolyte was composed of 10 mM CrO_3–2 mM hexamethonium bromide in 10% MeOH–water (pH 8.0) adjusted with triethanolamine. The background electrolyte was passed through a cellulose acetate membrane filter (0.2 μm). Prior to the first run, the capillary was rinsed with 0.1 M NaOH for 10 min, followed by washing with water for 10 min, and then filled with the background electrolyte. The capillary was conditioned by pre-electrophoresis (–20 kV) for 10 min. After washing the capillary with water and filling with the background electrolyte, samples were automatically injected using pressure injection mode at 1.0 psi for 10 s. Electrophoresis was performed at –20 kV using reverse polarity. Detection was carried out with monitoring the UV absorption at 254 nm. The negative peaks due to the presence of anions in the background of CrO_3 were automatically converted into positive peaks by Beckman 32 Karat software version 4.0 (Beckman Coulter).

Hydrolysis of Sulfated Carbohydrates

A standard solution (20 μL) of glucose 3-sulfate was mixed with 20 μL of 1 M HCl and the mixture was kept at 100°C in a polypropylene tube for specified times. After cooling the mixture to room temperature, the solution (40 μL) was diluted with 1000 μL of water. An aqueous solutions (1000 μL) of $NaNO_3$ was added to the mixture as internal standard and an aliquot (20 μL) was used for the analysis of sulfate ion.

Standard Procedure for the Determination of Sulfate Content in Sulfated Oligo- and Polysaccharides

A solution (20 μL) of sodium salt of sulfated oligo- or polysaccharides was mixed with 20 μL of 1 M HCl, and the mixture was kept at 100°C for 2 h. After cooling the mixture to room temperature, water and the internal standard solutions were added to the mixture as described above and an aliquot was used for the determination of sulfate ion. The content of sulfate ion was calculated from the calibration curve obtained from standard solutions of Na_2SO_4. The percentages of sulfate content were calculated using the following equation:

$$SO_3\,(w/w) = (\text{wt of } SO_4^{2-} \times (\text{wt of } SO_3/\text{wt of } SO_4)/\text{wt of sample}) \times 100$$

where wt (weight) of $SO_3 = 80$, wt of $SO_4^{2-} = 96$, wt of SO_4^{2-} (μg) in hydrolysates is the amount calculated using the calibration curve, and wt of the sample is the amount of the sample in micrograms.

Results and Discussion

Principle

The method is based on the acid hydrolysis of sulfonic acid ester (-O-SO_3H and -NH-SO_3H) followed by the determination of the released sulfate ion (SO_4^{2-}) with CE with indirect UV detection technique. Sulfated oligo-/polysaccharides are hydrolyzed with HCl to produce SO_4^{2-}. In CE, indirect detection is conveniently available for the detection of compounds which do not have chromophores/fluorophores. When non-UV absorbing sulfate ion passes through the UV detector, the zone of SO_4^{2-} causes a negative signal in the background electrolyte containing a UV-absorbing compound as probe. The output polarity of the detection is reversed so that a positive peak is obtained. The content of sulfate ester in parent compounds is calculated using the calibration curve obtained from a standard solution of Na_2SO_4.

Selection of the Background Electrolyte

Selection of the electrolyte (e.g. co-ion and electroosmotic modifier) is important for the sensitive and quantitative determination of sulfate ion. In the present study, chromate ion was selected as the UV absorbing co-ion (probe ion) because of its ionic mobility being close to that of SO_4^{2-}, which ensures high peak symmetry (Johns *et al.*, 2003; Pacakova *et al.*, 2003). We had to pay attention on the presence of high excess amount of chloride ion (Cl^-) in the sample solutions due to the HCl employed for the hydrolysis of sulfate-containing carbohydrates. Inorganic anions by CE are usually analyzed under negative polarity using electroosmotic modifiers such as cationic surfactant, polymer and amines, which improve resolutions of the ions (Haddad *et al.*, 1999; Harakuwe *et al.*, 1999; Kaniansky *et al.*, 1999). Muzikar *et al.* (2003) reported the determination of trace amount of inorganic anions (e.g. SO_4^{2-} or NO_3^-) in the presence of a large excess of Cl^- using an electrolyte consisting of triethanolamine (TEA)-buffered chromate with hexamethonium bromide (HMB) as electroosmotic modifier. In the present study, SO_4^{2-} (0.21 mM as Na_2SO_4) was successfully analyzed in the presence of 50 mM HCl using this condition, and Cl^- and SO_4^{2-} were completely resolved and observed at 4.50 and 4.85 min, respectively (Fig. 1a).

We employed nitrate ion (NO_3^-) as internal standard (50 μg/mL, 0.59 mM; Fig. 1b). Ions of SO_4^{2-} and NO_3^- with a huge amount of Cl^- were completely resolved within 5 min. Based on these results, 10 mM CrO_3–2 mM HMB in 10% MeOH–water (pH 8.0 adjusted with TEA) was selected as the background electrolyte throughout the present study.

(s): delete

Linearity and Limit of Detection

The calibration curve for absolute peak area of sulfate ion showed good linearity between 5.0 and 625 μg/mL ($y = 65.4x + 0.58$, $R = 0.9996$; Fig. 2a). In the case of correction of the injection amount by internal standard, the calibration curve exhibited excellent linearity ($y = 0.015x + 0.22$, $R = 0.9999$; Fig. 2b). Both lower limit of detection (LOD) and lower limit of quantification (LOQ) were evaluated on the basis of the standard deviation (σ) and slope (*S*) from the calibration curve of SO_4^{2-}. In the present conditions, LOD (= 3σ/S) and LOQ (= 10σ/S) were 0.934 and 3.113 μg/mL, respectively.

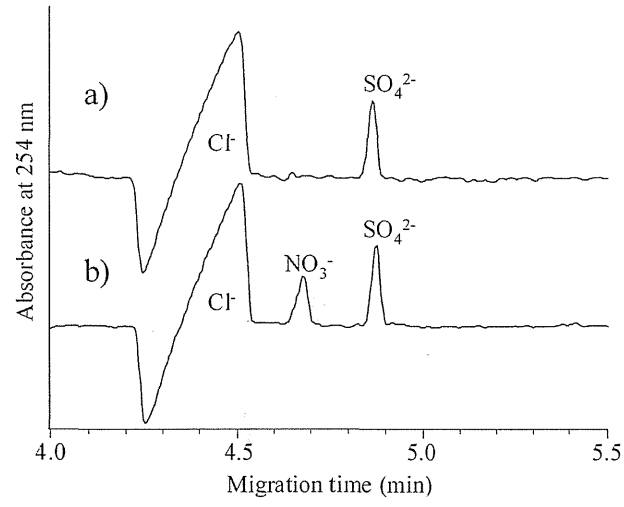

Figure 1. Separation of inorganic anions by CE with indirect UV detection: (a) 0.21 mM sulfate and 50 mM chloride; (b) 0.21 mM sulfate, 50 mM chloride, and 0.59 mM nitrate. Background electrolyte: 10 mM CrO_3/2 mM hexamethonium bromide in 10% MeOH–water at pH 8.0 adjusted with triethanolamine. Capillary: a fused silica capillary (i.d., 50 μm; effective length 56 cm). Applied voltage, –20 kV; temperature, 25 C; sample injection, hydrodynamic injection (1.0 psi, 10 s); detection, indirect UV absorption at 254 nm. [1]

°C

Reproducibility

Run-to-run reproducibility of migration times of SO_4^{2-} and NO_3^- was evaluated using a mixture of 30 μg/mL Na_2SO_4 and 50 μg/mL $NaNO_3$. Migration times of SO_4^{2-} and NO_3^- were 4.96 ± 0.08 and 4.68 ± 0.07, respectively. The relative standard deviation (RSD) was less than 1.4 and 1.6%, respectively ($n = 5$).

Precision

We obtained RSD values in absolute determination of SO_4^{2-} using standard solutions of Na_2SO_4 at 5, 30 and 312.5 μg/mL. The RSD (%) of SO_4^{2-} peak area were 4.58, 2.24 and 2.83%, respectively ($n = 5$; Table 1). In contrast, when using the internal standard (NO_3^-), the RSD (%) of SO_4^{2-} was 1.84, 0.69 and 1.69%, respectively ($n = 5$; Table 1).

Optimization of Conditions for Liberation of SO_4^{2-} by Acid Hydrolysis

Conditions for liberation of SO_4^{2-} from sulfated carbohydrates by acid hydrolysis with HCl were optimized using glucose 3-sulfate as model. After hydrolysis of glucose 3-sulfate with 1 M HCl at 100°C for specified intervals, a portion of the reaction mixture was diluted with water. An aqueous solution of the internal standard ($NaNO_3$) was added, and the released SO_4^{2-} was determined according to the conditions described above.

The content of SO_4^{2-} in the reaction mixture was dependent on hydrolysis time and the hydrolysis was completed within 2 h as shown in Fig. 3(a, b). The excess chloride ion and free glucose produced by hydrolysis in the mixture did not show interference in the determination of SO_4^{2-}. The amount of sulfate ion in glucose 3-sulfate was estimated as 28.1 w/w% (0.96 mol/mol), and showed good agreement with the theoretical values (28.4%). Recoveries were 95.9–96.7% ($n = 5$).

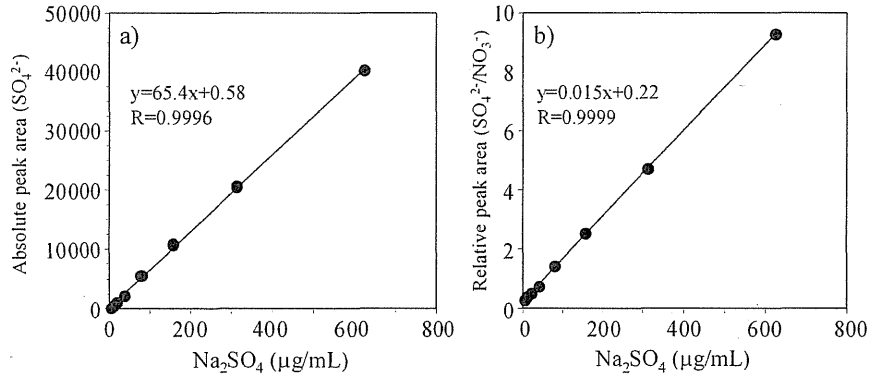

Figure 2. Calibration curve for determination of sulfate ions. (a) Concentration of Na_2SO_4 vs absolute peak area of SO_4^{2-}. (b) Concentration of Na_2SO_4 vs relative peak area (SO_4^{2-}/NO_3^-).

Table 1. Precision results of determination of sulfate ion at three different concentrations

Run	Peak area								
	5 μg/mL Na_2SO_4			30 μg/mL Na_2SO_4			312.5 μg/mL Na_2SO_4		
	SO_4^{2-}	NO_3^-	SO_4^{2-}/NO_3^-	SO_4^{2-}	NO_3^-	SO_4^{2-}/NO_3^-	SO_4^{2-}	NO_3^-	SO_4^{2-}/NO_3^-
1	462	361	1.280	2755	2043	1.349	28041	21505	1.304
2	492	378	1.302	2647	1957	1.353	29945	22869	1.309
3	506	402	1.259	2798	2092	1.337	28762	22214	1.295
4	476	362	1.315	2695	1989	1.355	27945	22290	1.254
5	518	409	1.267	2679	2008	1.334	29013	22452	1.292
Average	491	382	1.284	2715	2018	1.346	28741	22266	1.291
SD	22.5	22.3	0.024	60.8	51.9	0.009	813.6	495.1	0.022
RSD%	4.58	5.83	1.838	2.24	2.57	0.687	2.83	2.22	1.694

We evaluated linearity, repeatability, precision and lower limit of detection using sucrose octasulfate. Sucrose octasulfate is a cytoprotective drug widely used to prevent or treat several gastrointestinal diseases such as gastro-esophageal reflux, gastritis, peptic ulcer, stress ulcer and dyspepsia (Lam and Ching, 1994; Candelli *et al.*, 2000). The sulfate content found in the hydrolysate of sucrose octasulfate showed a good linear relationship with sucrose octasulfate (0.03–1 mg/mL). The value for the relative standard deviation ($n = 5$) of determination of sucrose octasulfate was 1.90% at 250 μg/mL. The limit of detection was 7.8 μg/mL as a solution of sucrose octasulfate sodium salt. When a solution (250 μg/mL) of sucrose octasulfate sodium salt was used, the sulfate content of one batch was 53.1% (accuracy 97.4–101.9%, $n = 5$), which is very close to the theoretical value (54.2%).

Determination of Sulfate Content in Various GAG Samples

Glycosaminoglycans (GAGs) are a family of highly complex and polydisperse linear polysaccharides that display a variety of important biological roles (Jackson *et al.*, 1991; Scott, 1992; Bourin and Lindahl, 1993; Sugahara and Kitagawa, 2000). GAGs are categorized into some main structural groups: hyaluronic acid (HA), chondroitin sulfate A (CSA), dermatan sulfate (DS), heparin (HP) and heparan sulfate (HS) (Zaia, 2009). The structural complexity is compounded by their sequence heterogeneity, primarily caused by variation of the degree and position of sulfate groups. We applied the present method to the determination of sulfate content in some GAG samples. The results are shown in Fig. 4 and Table 2.

Among five GAG samples used in the study, CSA, DS, HP and HS showed sulfate contents of 14.2, 15.0, 25.1 and 11.5%, respectively. HP is mainly composed of trisulfated disaccharide units, α(1-4)-linked L-iduronic acid, which is 2-*O*-sulfated, and D-glucosamine, which is *N*- and 6-*O*-sulfated (Zaia, 2009). Therefore, the sulfate content of HP is higher than those of CSA and DS, which are sulfated at only 4-OH of GalNAc in the disaccharide unit. The sulfate content of HS is lower than those of other sulfated GAGs, because HS from bovine kidney contains unsulfated repeating disaccharide units (GlcAβ1–4GlcNAc) as the major component (~60%), and contains the monosulfated GlcA β1–4GlcNAc (~25%) and the di- or tri-sulfated IdoAα1–4GlcNAc (~15%) (Zaia, 2009). HA, composed of non-sulfated disaccharide units, does not contain sulfate. When hydrolysis step was not included, we did not observe sulfate ions in the electropherograms for all these GAG samples (data not shown). This indicates that inorganic sulfate ion was negligible in the sample. The sulfate contents found in five GAGs were in good agreement with those calculated from sulfur contents provided by the manufacturer (Table 2).

Application to the Monitoring of Chemical Sulfation of Chondroitin Sulfate

Chemical modification of polysaccharides such as sulfation affords novel biological activity, and has been well studied (Srinivasan *et al.*, 1970; Suzuki *et al.*, 2001). We synthesized some preparations of sulfated chondroitin sulfate having different degree of sulfation by changing the amount of pyridine–sulfur

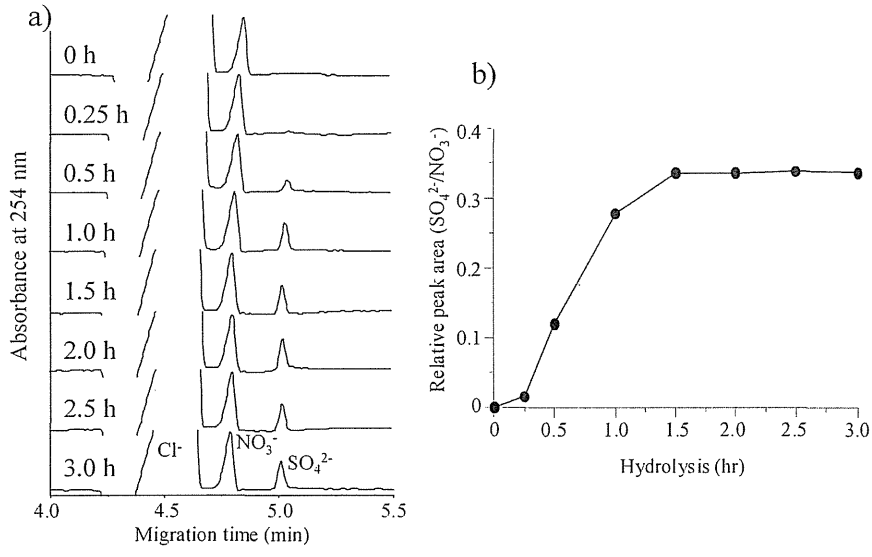

Figure 3. Time course of sulfate liberation during hydrolysis of the glucose 3-sulfate with HCl. (a) Electropherograms of the reaction mixture after hydrolysis. (b) Time course of liberation of sulfate ion from glucose 3-sulfate.

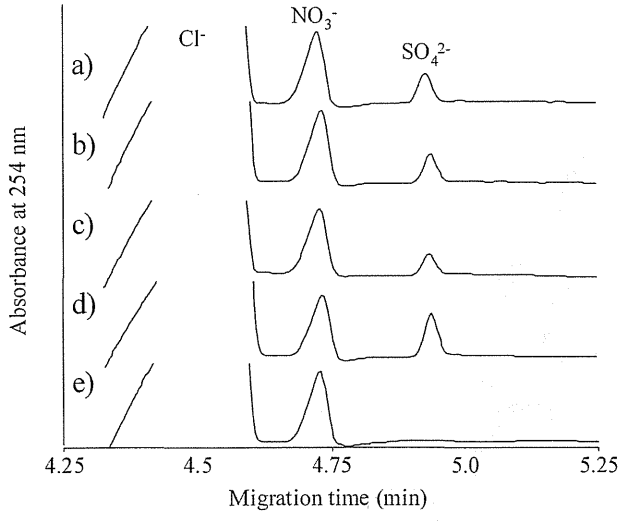

Figure 4. Determination of the sulfate content of some glycosaminoglycans. (a) Chondroitin sulfate A; (b) dermatan sulfate; (c) heparan sulfate; (d) heparin; and (e) hyaluronic acid.

pyridine-sulfur trioxide complex

complex according to the method reported by Maruyama *et al.* (1998). The $PSCS_{10}$, $PSCS_{50}$, $PSCS_{100}$ and $PSCS_{250}$ were obtained from 10 mg CS using 10, 50, 100, and 250 mg pyridine–sulfur complex, respectively. Each preparation was analyzed by the present technique (Table 3).

Sulfate contents calculated from the preparations of $PSCS_{10}$, $PSCS_{50}$, $PSCS_{100}$ and $PSCS_{250}$ were 24.7, 38.5, 45.5 and 48.09%, respectively. The results showed that the amount of pyridine–surfur trioxide complex used in the reaction caused remarkable differences in the sulfate contents, and showed that the present method is useful for monitoring the degree of sulfation during chemical sulfation of oligo-/polysaccharides.

Table 2. Sulfate contents of GAGs

GAGs	Total sulfate (%)[a]	
	Present method	Schoniger method[b]
Hyaluronic acid	n.d.[c]	<0.5
Chondroitin sulfate A	14.2 ± 0.5	15.0
Dermatan sulfate	15.0 ± 0.5	15.5
Heparin	25.1 ± 0.5	25.6
Heparan sulfate	11.5 ± 0.5	11.3

[a] Calculated from the dry weight of GAGs.
[b] Total sulfate contents were calculated from sufur contents provided by manufacturer.
[c] Not detected.

Conclusion

In the present study, we developed a simple, robust and reliable method for the determination of sulfate content in sulfated carbohydrates using CE with indirect UV detection. The background electrolyte consisting of TEA-buffered chromate with HMB is the most appropriate for the analysis of sulfate ion liberated from parent compounds after hydrolysis with HCl.

We applied the present method to the determination of sulfate content in some sulfated GAG samples such as chondroitin sulfate, dermatan sulfate, heparin and heparan sulfate. The sulfate contents found in these GAGs were in good agreement with those obtained by conventional methods. We also applied the method to the determination of sulfate content in chemically sulfated chondroitin sulfate, and revealed the degree of sulfation.

Easy operation of the proposed technique is useful for the determination of sulfate content of sulfated oligo-/polysaccharides. The present method is suitable for routine analysis of sulfate content of carbohydrates.

Table 3. Sulfate contents of chemically sulfated chondroitin sulfate

Sample	Amount of pyridine–sufur trioxide complex	Total sulfate content (%)	Degree of sulfation (%)[b]
CSA[a]	—	14.2	27.5
$PSCS_{10}$	10 mg	24.7	47.6
$PSCS_{50}$	50 mg	38.5	74.6
$PSCS_{100}$	100 mg	45.5	88.2
$PSCS_{250}$	250 mg	48.1	93.2

[a] Chondroitin sulfate A from whale cartilage.
[b] Relative percentage to theoretical value (51.6%) of fully sulfated CSA-30mer.

References

Bourin MC and Lindahl U. Glycosaminoglycans and the regulation of blood coagulation. *Biochemistry Journal* 1993; **289**(Pt 2): 313–330.

Candelli M, Carloni E *et al.* (2000). Role of sucralfate in gastrointestinal diseases. *Panminerva Medicine* 2000; **42**(1): 55–59.

Cole DE, Evrovski J. Quantitation of sulfate and thiosulfate in clinical samples by ion chromatography. *Journal of Chromatography A* 1997; **789**(1–2): 221–232.

Fritz JS. Recent developments in the separation of inorganic and small organic ions by capillary electrophoresis. *Journal of Chromatography A* 2000; **884**(1–2): 261–275.

Giangrande PL. Fondaparinux (Arixtra): a new anticoagulant. *International Journal of Clinical Practice* 2002; **56**(8): 615–617.

Haddad PR, Doble P *et al.* Developments in sample preparation and separation techniques for the determination of inorganic ions by ion chromatography and capillary electrophoresis. *Journal of Chromatography A* 1999; **856**(1–2): 145–177.

Harakuwe AH, Haddad PR *et al.* Effect of drying on the degradation of cationic surfactants and separation performance in capillary zone electrophoresis of inorganic anions. *Journal of Chromatography A* 1999; **863**(1): 81–87.

Hattori K, Yoshida T *et al.* Synthesis of sulfonated amino-polysaccharides having anti-HIV and blood anticoagulant activities. *Carbohydrate Research* 1998; **312**(1–2): 1–8.

Hemmerich S and Rosen SD. 6′-sulfated sialyl Lewis x is a major capping group of GlyCAM-1. *Biochemistry* 1994; **33**(16): 4830–4835.

Honke K and Taniguchi N. Sulfotransferases and sulfated oligosaccharides. *Medical Research Review* 2002; **22**(6): 637–654.

Hooper LV, Manzella SM *et al.* From legumes to leukocytes: biological roles for sulfated carbohydrates. *FASEB Journal* 1996; **10**(10): 1137–1146.

Jackson RL, Busch SJ *et al.* Glycosaminoglycans: molecular properties, protein interactions, and role in physiological processes. *Physiology Review* 1991; **71**(2): 481–539.

Johns C, Macka M *et al.* Enhancement of detection sensitivity for indirect photometric detection of anions and cations in capillary electrophoresis. *Electrophoresis* 2003; **24**(12–13): 2150–2167.

Kaniansky D, Masar M *et al.* Capillary electrophoresis of inorganic anions. *Journal of Chromatography A* 1999; **834**(1–2): 133–178.

Katsuraya K, Ikushima N *et al.* Synthesis of sulfated alkyl malto- and laminara-oligosaccharides with potent inhibitory effects on AIDS virus infection. *Carbohydrate Research* 1994; **260**(1): 51–61.

Katsuraya K, Nakashima H *et al.* Synthesis of sulfated oligosaccharide glycosides having high anti-HIV activity and the relationship between activity and chemical structure. *Carbohydrate Research* 1999; **315**(3–4): 234–242.

Lam SK and Ching CK. Sucralfate in clinical practice. *Journal of Gastroenterology and Hepatology* 1994; **9**(4): 401–411.

Lindahl U, Backstrom G *et al.* The antithrombin-binding sequence in heparin. Identification of an essential 6-O-sulfate group. *Journal of Biological Chemistry* 1983; **258**(16): 9826–9830.

Lopez-Ruiz B. Advances in the determination of inorganic anions by ion chromatography. *Journal of Chromatography A* 2000; **881**(1–2): 607–627.

Maruyama T, Toida T *et al.* Conformational changes and anticoagulant activity of chondroitin sulfate following its O-sulfonation. *Carbohydrate Research* 1998; **306**(1–2): 35–43.

Muzikar M, Havel J *et al.* Capillary electrophoresis determinations of trace concentrations of inorganic ions in large excess of chloride: soft modelling using artificial neural networks for optimisation of electrolyte composition. *Electrophoresis* 2003; **24**(12–13): 2252–2258.

Pacakova V, Coufal P *et al.* The importance of capillary electrophoresis, capillary electrochromatography, and ion chromatography in separations of inorganic ions. *Electrophoresis* 2003; **24**(12–13): 1883–1891.

Paull B and King M. Quantitative capillary zone electrophoresis of inorganic anions. *Electrophoresis* 2003; **24**(12–13): 1892–1934.

Roy AB and Turner J. The sulphatase of ox liver. XXIV. The glycosulphatase activity of sulphatase a. *Biochimica Biophysica Acta* 1982; **704**(2): 366–373.

Saillard S, Gareil P *et al.* Development of a capillary electrophoresis assay based on free sulfate determination for the direct monitoring of sulfoesterase activity. *Analytical Biochemistry* 1999; **275**(1): 11–21.

Scott JE. Supramolecular organization of extracellular matrix glycosaminoglycans, *in vitro* and in the tissues. *FASEB Journal* 1992; **6**(9): 2639–2645.

Small DH, Mok SS *et al.* Role of proteoglycans in neural development, regeneration, and the aging brain. *Journal of Neurochemistry* 1996; **67**(3): 889–899.

Srinivasan SR, Radhakrishnamurthy B *et al.* Determination of sulfate in glycosaminoglycans by gas–liquid chromatography. *Analytical Biochemistry* 1970; **35**(2): 398–404.

Sugahara K and Kitagawa H. Recent advances in the study of the biosynthesis and functions of sulfated glycosaminoglycans. *Current Opinion on Structural Biology* 2000; **10**(5): 518–527.

Suzuki A, Toyoda H *et al.* Preparation and inhibitory activity on hyaluronidase of fully O-sulfated hyaluro-oligosaccharides. *Glycobiology* 2001; **11**(1): 57–64.

Tadano-Aritomi K, Hikita T *et al.* Determination of lipid-bound sulfate by ion chromatography and its application to quantification of sulfolipids from kidneys of various mammalian species. *Journal of Lipid Research* 2001; **42**(10): 1604–1608.

Terho TT and Hartiala K. Method for determination of the sulfate content of glycosaminoglycans. *Analytical Biochemistry* 1971; **41**(2): 471–476.

Timerbaev AR. Recent advances and trends in capillary electrophoresis of inorganic ions. *Electrophoresis* 2002; **23**(22–23): 3884–3906.

Timerbaev AR. Capillary electrophoresis of inorganic ions: an update. *Electrophoresis* 2004; **25**(23–24): 4008–4031.

Toida T, Maruyama T *et al.* Preparation and anticoagulant activity of fully O-sulphonated glycosaminoglycans. *International Journal of Biology and Macromoles* 1999; **26**(4): 233–241.

Tsuboi S, Isogai Y *et al.* 6′-Sulfo sialyl Lex but not 6-sulfo sialyl Lex expressed on the cell surface supports L-selectin-mediated adhesion. *Journal of Biological Chemistry* 1996; **271**(44): 27213–3716.

Villanueva GB. Predictions of the secondary structure of antithrombin III and the location of the heparin-binding site. *Journal of Biological Chemistry* 1984; **259**(4): 2531–2536.

Werz DB and Seeberger PH. Carbohydrates as the next frontier in pharmaceutical research. *Chemistry* 2005; **11**(11): 3194–3206.

Wu XZ. Sulfated oligosaccharides and tumor: promoter or inhibitor? *Panminerva Medicine* 2006; **48**(1): 27–31.

Yoshida T, Yasuda Y *et al.* Synthesis of curdlan sulfates having inhibitory effects *in vitro* against AIDS viruses HIV-1 and HIV-2. *Carbohydrate Research* 1995; **276**(2): 425–436.

Zaia J. On-line separations combined with MS for analysis of glycosaminoglycans. *Mass Spectrometry Review* 2009; **28**(2): 254–272.

